UNIVERSITY OF TURKU

Association between TSPO-PET measurable microglial activation and plasma CHI3L1 in multiple sclerosis

Faculty of Medicine, Institute of Biomedicine
MDP in Biomedical Sciences, Drug Discovery and Development
Master's thesis

Author:
Venla Ahola

Supervisors:
Professor, MD, PhD Laura Airas
PhD Maija Saraste

3.5.2024
Turku

Master's thesis

Subject: Drug Discovery and Development
Author(s): Venla Ahola
Title: Association between TSPO-PET measurable microglial activation and plasma CHI3L1 in multiple sclerosis
Supervisor(s): Professor, MD, PhD Laura Airas, PhD Maija Saraste
Number of pages: 63 pages
Date: 3.5.2024

BACKGROUND Multiple sclerosis (MS) is the most common disabling central nervous system (CNS) disease affecting young adults, especially women. Neurologic symptoms result from inflammatory lesions in brain, spinal cord and optic nerve caused by immune cell infiltration from periphery into brain promoting inflammation, demyelination, gliosis, and neuroaxonal degeneration. Diffuse inflammation across brain, caused by activation of CNS-resident cells, microglia and astrocytes, contributes to disease progression throughout the disease course. Several effective treatments for relapsing-remitting MS (RRMS) are currently available but only few for progressive MS (PMS). Clinical course varies considerably between patients; hence, there is an urgent need for biomarkers. Chitinase-3 like-protein-1 (CHI3L1) is one potential biomarker. In the brain, CHI3L1 participates in neuroinflammatory processes and is produced by activated astrocytes and microglia. Microglial activation can be detected *in vivo* using TSPO-PET.

MATERIALS AND METHODS Study cohort consisted of 54 MS patients (25 progressive MS [PMS] and 29 relapsing-remitting MS [RRMS]) and 17 healthy controls (HCs). TSPO-PET imaging using [^{11}C]PK11195-ligand and blood sampling were conducted concurrently. CHI3L1 was measured with commercial ELISA-kit from plasma samples. Additionally, clinical evaluation and magnetic resonance imaging (MRI) were performed.

RESULTS Plasma CHI3L1 concentration was increased in MS compared to HCs (median 20.9 ng/ml vs. 16.8 ng/ml; $p = 0.0497$). CHI3L1 concentration was significantly higher in PMS than in HC (23.5 ng/ml vs. 16.8 ng/ml; $p = 0.0055$). There was a correlation between specific [^{11}C]PK11195-binding, presented as brain distribution volume ratio (DVR), and CHI3L1 plasma concentration in MS patients (Spearman correlation, $r = 0.31$, $p = 0.049$) and in PMS patients ($r = 0.56$, $p = 0.0499$). Additionally, CHI3L1 concentration correlated with brain volume in both MS ($r = -0.38$, $p = 0.0051$) and PMS ($r = -0.49$, $p = 0.013$), but not with MS related clinical variables such as disease duration and the Expanded Disability Status Scale (EDSS). Notably, CHI3L1 concentration correlated strongly with age ($r = 0.39$, $p = 0.0035$) in MS cohort but not in PMS ($p = 0.13$) cohort.

CONCLUSIONS Correlation between CHI3L1 and microglial activation in brain suggests that CHI3L1 is a promising biomarker for MS progression related pathology and smouldering inflammation.

Key words: CHI3L1, Microglia, Multiple Sclerosis, TSPO-PET

Table of contents

1 Introduction

1.1 Multiple Sclerosis

Multiple sclerosis (MS) is the most common chronic inflammatory disease of the central nervous system (CNS) typically affecting young adults. The disease is at least two times more common in women than in men and the typical age of the diagnosis is 20-40 years. Characteristic symptoms of MS include monocular visual loss due to optic neuritis, limb weakness or sensory loss, double vision, and ataxia. However, symptoms vary a lot and depend largely on the location of the inflammation. In most cases, symptoms occur irregularly and worsen over the years leading to progressive impairment of mobility and cognition. In early stages of the disease, symptoms result from local inflammation in brain, spinal cord, and optic nerve causing demyelination, the damage of myelin sheath in dendrites and axons. (Reich et al., 2018) When disease progresses, diffuse inflammation outside lesions becomes to prevail. Concomitant inflammation throughout the CNS drives disease progression and is followed by a cascade of damaging events such as production of reactive oxygen species (ROS) and reactive nitrogen species (RNS) both of which further promote mitochondrial injury (Dendrou et al., 2015).

MS is diagnosed based on specific instructions known as the McDonald criteria. Diagnosis is a combination of clinical, imaging, and laboratory findings. Magnetic resonance imaging (MRI) evidence of dissemination in time and space are gathered to exclude other neurological conditions. New clinical relapses connected to lesions seen in MRI at different points over time are considered as evidence of dissemination in time and multiple lesion locations in brain or spinal cord indicates dissemination in space. In practice, this means that if a patient has had both 2 or more clinical attacks and 2 or more lesions in different locations, there is evidence of both dissemination in time and space and diagnosis can be set. Additional lumbar puncture to detect cerebrospinal fluid (CSF)-specific oligoclonal bands can be obtained in cases where only one clinical attack can be demonstrated. (Thompson et al., 2018)

MS is divided into several clinical subtypes: clinically isolated syndrome (CIS), relapsing-remitting MS (RRMS), secondary progressive MS (SPMS) and primary progressive MS (PPMS). RRMS is the most typical clinical subtype comprising over 80% of the MS patients. RRMS can be identified as a subtype in which relapses (episodes of neurological dysfunction

lasting at least 24h in the absence of fever or infection) occur and are followed by periods of remission. If only one relapse has occurred, the disease is determined as CIS. Majority of the RRMS patients develop gradually, after 15-20 years of disease manifestation, SPMS, where relapses occur less frequently but the disability worsening continues progressively. PPMS, comprising approximately 10% of MS patients, is characterized by slowly progressive increase in neurological disability from the onset of the disease usually without relapses. (Brownlee et al., 2017)

EDSS (Expanded Disability Status Scale) scores are employed to assess the severity and progression of the MS disease. To determine EDSS score, patient's muscle weakness and ability to move arms and legs, balance, coordination and tremor, eye movements, speech and swallowing, unusual sensations and numbness, bowel and bladder function, eyesight, and thinking and memory are evaluated. EDSS has a range from 0 to 10 indicating the effect of the disease on the patient's functional capacity. The higher the score the higher the level of disability. Score 0 indicates zero disability and 10 death due MS. (Kurtzke, 1983)

The risk factors for MS disease are not fully known despite extensive research work, yet various genetic and environmental risk factors have been proposed. Most dominant risk factors include obesity, cigarette smoking, low vitamin D levels, female sex, and Epstein-Barr virus (EBV) and other viruses. It has been shown by longitudinal analysis of over 10 million young adults, that EBV has an important role in the pathogenesis of MS. The infection increases the risk of developing MS 32-fold (Bjornevik et al., 2022). However, very few of those infected with EBV develop MS and no other viruses have been proven to initiate the disease. Three-quarters of MS patients are women, but the reason is still unknown, although it is common that women are more susceptible to autoimmune diseases in general. First-degree relatives of MS patients have 2-4% risk for developing MS (vs. general population ~ 0.1%) and monozygotic twins 30-50%. (Reich et al., 2018)

Genome-wide studies have identified over 200 gene variants that increase the risk to MS most of which are associated with immune-pathways. One of the associated loci is the human leukocyte antigen (HLA) DRB1*15:01 haplotype. (Reich et al., 2018) Some others include HLA-A*02:01, and the genes encoding IL-7 and IL-2 receptors thus altering the cytokine homeostasis. There are also other MS-associated genetic polymorphisms that primarily affect

the immune cell activation and are partially shared with other autoimmune diseases. (Dendrou et al., 2015)

Over the years, several disease modifying treatment alternatives have been developed for RRMS, but none of them fully prevents or reverses progressive MS (PMS). The medication for RRMS reduces the relapses and inflammation seen in MRI and thus, by reducing the disease burden, they can prevent the impairment of mobility and functional ability in the long run. PMS however lacks effective treatment. The inflammatory activity in RRMS is controllable by disease-modifying treatments, but when disease progresses, the underlying pathogenesis leading to neurodegeneration that drives clinical progression and accumulation of disability, changes and the treatments are not anymore able to prevent or delay this degeneration (Thompson and Ciccarelli, 2020). Yet one treatment, ocrelizumab, has been shown to be efficacious in slowing disease progression in PPMS and one, siponimod, in SPMS. (Montalban et al., 2017; Kappos et al., 2018)

1.2 Pathology of MS

With or without an exogenous triggering factor, ongoing disease eventually leads to focal and diffuse pathological signs of MS; neuroaxonal loss, brain atrophy and ventricular enlargement. The most typical pathological findings in MS are demyelinated areas, called lesions or plaques, in the white and grey matter of the brain and spinal cord. The most common lesion type in early MS, the focal white matter demyelinating lesion, is typically located around the ventricles, the optic nerves and tracts, the corpus callosum, the cerebellar peduncles, the long tracts, and in the spinal cord and brainstem. MS lesions can be classified based on their activation status and prevalence of immune cells in them. Different lesion types are illustrated in Figure 1. (Pukoli and Vécsei, 2023)

Acute active lesions are most common in early MS, and their proportion gradually decreases when the disease progresses. Blood-brain-barrier (BBB) leakage and active demyelination are characteristic features of acute active lesions. Most of the acute lesions in MS eventually transform into chronic inactive lesions and shrink as a consequence of gliosis. (Pukoli and Vécsei, 2023) However, after approximately 10 years disease duration, when disease progresses, some lesions develop into slowly expanding lesions also called smouldering, chronic active, or mixed active-inactive lesions (Kuhlmann et al., 2017). At the cellular level,

these lesions are characterized by an inactive center containing lymphocytes but lacking macrophages and an active rim surrounding the lesion containing activated microglia/macrophages (Zrzavy et al., 2017; Böttcher et al., 2020). Smouldering lesions show axonal damage and demyelination and grow towards normal appearing white matter (NAWM) over time. In numerous imaging studies, it has been demonstrated that smoldering lesions are associated with worse prognosis and change from RRMS to PMS (Nylund et al., 2022; Datta et al., 2017; Sucksdorff et al., 2020). In some acute and chronic active lesions, iron accumulation is apparent in microglia and macrophages indicating pro-inflammatory status and more destructive type of lesion (Absinta et al., 2019). Smouldering lesions containing iron are called paramagnetic rim lesions (PRLs) or iron rim lesions (IRLs).

All pathological signs of MS are present in all stages of the disease, but the proportion of the features varies in different stages of the disease and between patients. Diffuse pathology seen as low-grade microglial inflammation outside lesions becomes to prevail along with disease progression. (Bodini et al., 2021) Diffuse pathology consists of perivascular inflammatory infiltrates, moderate brain edema, diffuse microglial activation, diffuse axonal injury, and astrocytic gliosis. Part of it happens as a secondary phenomenon to axonal and neuronal destruction in focal lesions and the other part develops independently without effect of focal lesions. (Lassmann, 2018) Neurodegeneration is present already from the early disease and has a central role in pathogenesis throughout the disease course (Kawachi and Lassmann, 2017). The mechanisms contributing to neurodegeneration and neuronal death can be divided into intra-neuronal and extra-neuronal processes. Intraneuronal processes include oxidative stress responses, energy deficiencies, and ionic homeostasis deficits. The most important extra-neuronal process, activation of the adaptive and innate immune systems is described in more detail in Chapters 1.2.1 and 1.2.2 and in Figure 1.

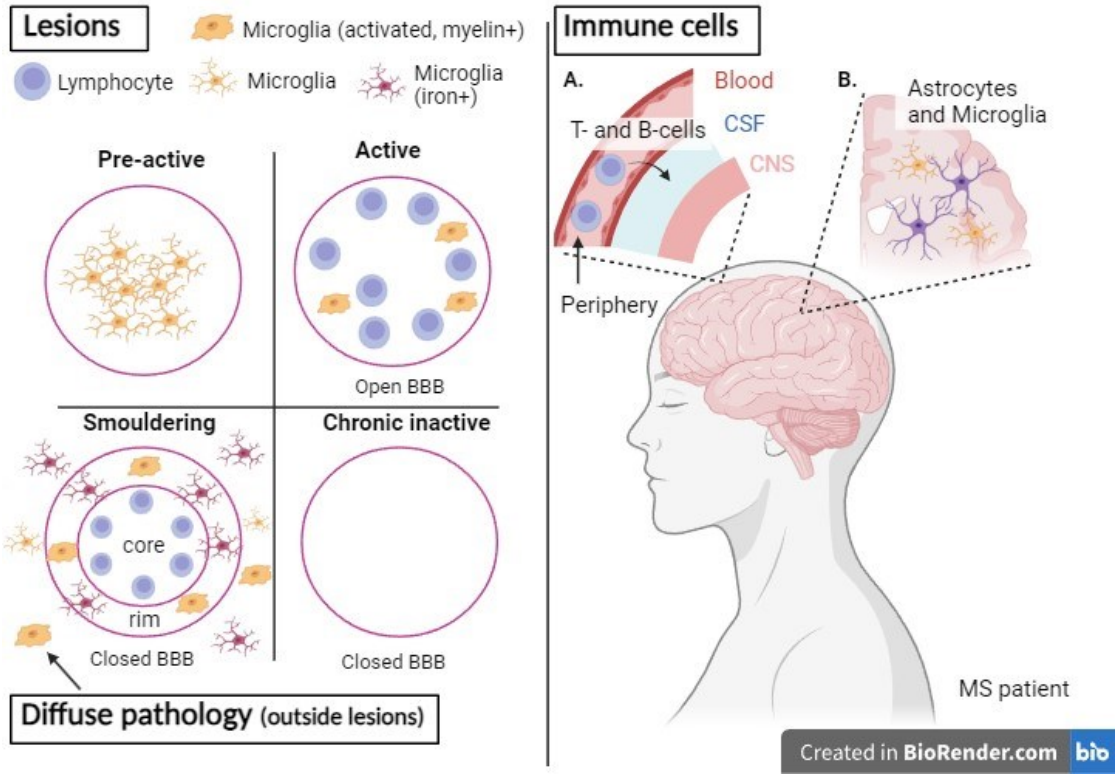

Figure 1. Pathology of MS. On the left side of the illustration, different types of lesions are presented. Pre-active lesion: Before lesion formation, microglia/macrophages proliferate and aggregate into a cluster. Active lesion: In the site of active lesion, there is active demyelination and microglia/macrophages contain phagocytosed myelin. Active lesions also contain infiltration of lymphocytes around central vein. Microglia/macrophages are activated and produce inflammatory cytokines. These kinds of lesions are most prominent in early MS. In addition, there is a significant damage to the blood-brain barrier (BBB). Smouldering lesions (chronic active, mixed active-inactive): These lesions comprise low-grade chronic inflammation and axonal damage with demyelination. Typical for smouldering lesions is increase in size. Some of these lesions contain iron-loaded activated microglia at the rim of the lesion and form paramagnetic rim lesions (PRLs)/iron rim lesions (IRLs). Chronic inactive lesions lack microglial cells and BBB is closed. On the right side of the illustration the MS pathology inside brain is described. A. In early MS, autoreactive lymphocytes traffic from periphery and begin to damage axons by recognizing antigens on the surface of them. B. When disease progresses, microglia and astrocytes activate and start to promote inflammation and tissue damage. *Left side of the figure is modified from* Pukoli and Vécsei, 2023. *For clarity, the term microglia is used but proper term would be microglia/macrophages. BBB; blood-brain-barrier; CNS, central nervous system; CSF, cerebrospinal fluid; MS, multiple sclerosis. Created in Biorender.*

1.2.1 Peripheral immune cells as part of immunopathology in MS

The fundamental factor initiating MS pathogenesis cascade and whether the factor comes from periphery or CNS remains unknown. Autoreactive T cells trafficking from periphery to CNS are possible triggering factors, but they may as well serve as a secondary phenomenon. T cells

are responsible for damaging axons, myelin-producing glia cells (oligodendrocytes), and BBB by recognizing antigens on the surface of these cells and by producing cytotoxic molecules. Additionally, they are able to inactivate "normal" T cells further promoting disease development. (Pukoli and Vécsei, 2023) It has been shown in MS patients and healthy controls (HCs) that myelin protein derived antigens, i.e. myelin basic protein (MBP), proteolipid protein, and myelin oligodendrocyte glycoprotein (MOG), are recognized by circulating CD4+ T cells highlighting the role of autoreactive T cells in MS pathogenesis since demyelination is a central pathological mechanism in MS (Hellings et al., 2001).

Th17 cells are an important T cell line considering MS pathogenesis, since they produce IL-17 which increases neutrophil migration, endothelial permeability and activation of microglia, macrophages, and astrocytes. Additionally, Th1 cells producing pro-inflammatory cytokine interferon-γ have a role in MS pathogenesis. Accordingly, multiple first-line disease-modifying MS therapeutics have been designed to block T cell differentiation towards Th1 cells which substantiates their central role in MS pathogenesis. In addition to CD4+ Th cells, CD8+ T cells participate in MS pathogenesis. Neuropathological studies have found CD8+ T cells in white matter and cortical grey matter lesions, and they correlate with axonal damage in post-mortem MS brain (Frischer et al., 2009). The involvement of CD8+ T cells in MS pathogenesis is not completely understood and requires more research in the future. Regulatory T cells are also considered central in MS pathogenesis because they inhibit the activation of autoimmune T and B cells (Dendrou et al., 2015).

B cells along with autoreactive T cells and monocytes traffic from periphery to CNS but contrary to T cells, the amount of B cells in CNS changes during the disease progression and increases along with aging. Based on pathological studies, the number of B cells is increased in the brain of patients with PPMS and SPMS (Frischer et al., 2009). Currently, there are couple of therapeutics targeting B cells by CD20-targeted monoclonal antibodies. Considering the number of immunotherapies that reduce infiltration or proliferation of lymphocytes, damage these cells or their cytokine production, it is evident that adaptive immune system is in key role especially in the early stages of MS pathogenesis.

1.2.2 Microglia and astrocytes as part of immunopathology in MS

Microglia and other CNS macrophages are mononuclear phagocytes that form from their progenitors during embryogenesis thus differing from monocyte-derived macrophages that are

formed throughout postnatal life in bone marrow and then enter the CNS through BBB in case of an insult (Zrzavy et al., 2017). Microglia have several critical biological functions in healthy brain including maintaining CNS homeostasis, participation into learning and memory, clearance of damaged elements and defense against insults. (Airas and Yong, 2022)

In healthy brain, microglia present a ramified morphology and constantly observe their surroundings. With persistence of threat, microglial activation occurs as a response to cytokines and chemokines. When activated, microglia transform from ramified morphology to ameboid-like cells and lose homeostatic characteristics. Activated microglia can be further divided into pro-inflammatory M1 microglia and anti-inflammatory M2 microglia (Tang and Le, 2016). However, based on current understanding, this division is probably too simple, as microglial activation is a complex process with numerous functional states and phenotypes (Ransohoff, 2016).

The distinction of different activation states of microglia would be important since this might help to clarify the pathological mechanisms relevant for disease progression. In brain tissue samples, microglial activation and lose of homeostatic characteristics can be visualized using immunohistochemistry. Activated microglia, with less ramified morphology, are present already in the early evolution of an MS lesion, in NAWM, before a lesion has formed. Thereafter, the density of microglia/macrophages increases along with the disease progression. (Airas and Yong, 2022). It was shown that in NAWM there is a reduction of homeostatic microglia in MS brain compared to healthy controls when P2RY12 purinergic receptor expressed by homeostatic microglia was stained. Instead, increase of activated, pro-inflammatory microglia, was seen in MS NAWM compared to HC NAWM. The degree of microglial activation increased with age in HCs and with disease progression in MS. Additionally, MS patients had a significant loss of homeostatic microglia in active lesion stages whereas homeostatic microglia appeared in inactive lesions. (Zrzavy et al., 2017). In addition to white matter lesions, microglial activity has also been found from cortical grey matter lesions (Kooi et al., 2012).

In the early disease states of MS, microglial cells may have a beneficial role, as they phagocyte myelin debris, which promotes the repairing process of myelin damage (Lampron et al., 2015). However, constant, and prolonged activation of microglia begins to induce damage to neurons and oligodendrocytes through various released molecules such as inflammatory cytokines

(TNF-α, IL-1β), glutamate, matrix metalloproteases and other proteases. Additionally, microglia have a high capacity to generate free radicals and they participate in regulating the iron homeostasis thus further inducing neurotoxicity. (Masuda et al., 2019; Airas and Yong, 2022) This is supported by a finding that accumulation of microglia/macrophages is correspondent with elevated axonal injury *in vivo* in EAE model and in postmortem MS brain (Howell et al., 2010).

Since macrophages and microglia are relatively difficult to distinguish, thorough studies are needed to identify their distinct roles (Dendrou et al., 2015). Microglia and macrophages comprise over 80% of immune cells in actively demyelinating lesions determined in post-mortem MS brain. Using microglia marker TMEM119, it has been identified that average of 45% of them are microglia and remaining half monocyte-derived macrophages (Zrzavy et al., 2017). In RRMS, myeloid cells in active lesions are mainly macrophages when in PMS, in slowly expanding lesions they are mainly microglia, often containing iron and correlating with axonal injury (Jäckle et al., 2020; Böttcher et al., 2020). The domination of monocyte-derived macrophages promoting demyelination in early MS has also been shown in experimental autoimmune encephalomyelitis (EAE), a common mouse model of MS, whereas microglia has been shown participate more in debris clearing (Yamasaki et al., 2014). Additionally, this same phenomenon has been shown in a post-mortem study. In classical active MS lesion core, microglial cells are mostly anti-inflammatory and attempts of remyelination are frequent. These neuroprotective microglia are almost absent in slowly expanding lesions suggesting a domination of pro-inflammatory microglia. (Zrzavy et al., 2017).

Astrocytes are resident glial cells of the CNS that participate in tissue injury repairing (Healy et al., 2022). They have an important role in CNS barrier functioning since they form glia limitants that line the neuronal tissue (Dendrou et al., 2015). Additionally, they function together with microglia by activating each other through production of chemokines and cytokines. Furthermore, astrocytes participate in many processes in brain including regulation of the BBB function, secretion and uptake of neurotransmitters, and the regulation of extracellular ion homeostasis (Connolly et al., 2023). Similar to microglia, astrocytes have a role as both pro-inflammatory and anti-inflammatory factors in MS brain. Additionally, researchers have found in CSF a positive correlation between astrocyte marker glial fibrillary acidic protein (GFAP) and microglia marker soluble triggering receptor expressed on myeloid

cells-2 (sTREM-2) and inflammatory cytokines which strengthens the assumption of microglia and astrocytes' concurrent effect in the CNS inflammation in MS (Azzolini et al., 2022).

1.3 Imaging methods in MS

1.3.1 MRI

MRI is a non-invasive imaging method producing three dimensional (3D) images which are often used for disease detection, diagnosis, and treatment monitoring. Conventional MRI used in diagnosis and follow-up in MS includes T2-weighted, fluid-attenuated inversion recovery (FLAIR) and T1-weighted pre- and post-gadolinium contrast pulse sequences. (Hemond and Bakshi, 2018) Conventional MRI is widely used in MS, in both clinical setting and Phase II treatment trials to demonstrate the central pathological features of MS such as location, morphology, number, and enhancement of lesions, and atrophy. (Gill et al., 2023) Examples of both T2-weighted FLAIR and T1-weighted images of MS brain are presented in Figure 2.

Gadolinium enhancement on MRI illustrates an actively disturbed BBB allowing the infiltration of peripheral immune cell from periphery into the CNS. Gadolinium enhanced acute lesions are typical especially in the early phases of MS (Gill et al., 2023). Iron rim lesions, i.e. chronic active lesions with an iron rim, can be detected with advanced MRI sequences such as susceptibility weighted imaging (SWI), T2*, and quantitative susceptibility mapping (QSM)(Dal-Bianco et al., 2017; Bagnato et al., 2024). Iron rims are relatively specific for MS disease though only about half of MS patients have at least one iron rim lesion. Chronic active white matter lesions surrounded by iron rims containing microglia recounts a more destructive MS disease and they do not enhance when gadolinium is administered underlining their chronic nature rather than active (Gill et al., 2023; Airas and Yong, 2022). Central vein sign (CVS) is one marker of MS that can be detected with MRI. CVS can be used to differentiate MS from similar diseases but not to differentiate between MS subtypes (Gill et al., 2023). Furthermore, brain atrophy, spinal cord atrophy, cortical lesions, enlarged perivascular spaces, and leptomeningeal enhancement seen in MRI can be used in MS prognosis. CNS atrophy, global and regional, is a marker of neurodegeneration and it is typical for MS patients, but it occurs also during aging. (Chataway et al., 2024)

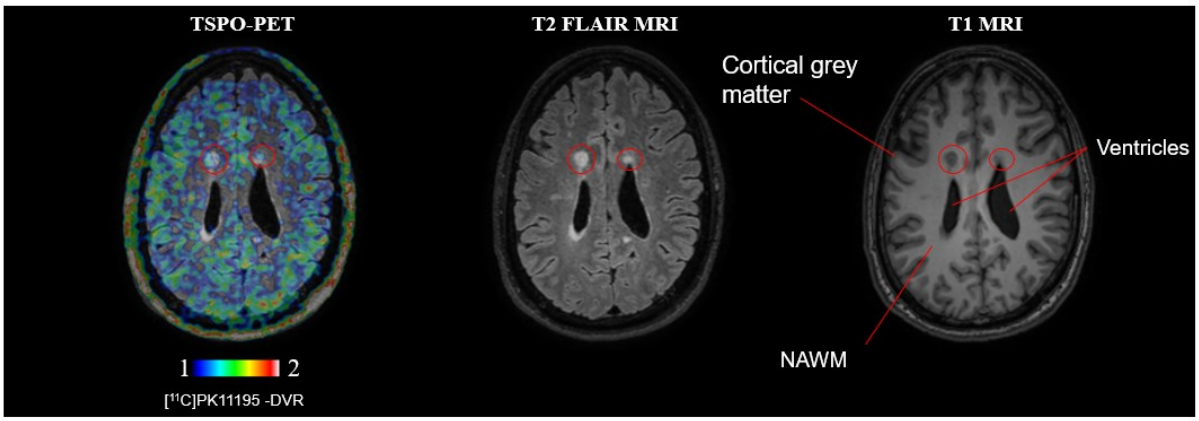

Figure 2. Examples of brain TSPO-PET and MRI images in MS. An image of a 40-year-old male RRMS patient with EDSS 1 imaged with 3T MRI and TSPO-PET. Left image represents a [^{11}C]PK11195 TSPO-PET image overlaid with T2 FLAIR image. The higher DVR represents [^{11}C]PK11195-binding indicating increased microglial activation. In MS, higher microglial activity can be seen in some lesions and in normal appearing white matter (NAWM) and in normal appearing grey matter (NAGM). Typical MS white matter lesions (red circles) around ventricles can be seen as hyperintense light ovoidal shaped spots in T2-weighted FLAIR MRI image and as hypointense dark spots in T1-weighted MRI image. Grey matter is seen as darker and NAWM as lighter in T1-weighted MRI image. *DVR, Distribution volume ratio; FLAIR, Fluid-Attenuated Inversion Recovery; MRI, Magnetic resonance imaging; NAWM, Normal appearing white matter; PET, Positron emission tomography.*

1.3.2 TSPO-PET

While conventional MRI is sensitive in demonstrating focal inflammatory lesions, it is not sensitive enough to illustrate the diffuse pathology outside focal lesions associated with MS progression. Positron emission tomography (PET) provides targeted, quantitative, and non-invasive imaging of physiological and pathological processes *in vivo.* PET method enables imaging of heterogenic MS lesions and inflammatory changes in NAWM and GM, but also functional changes in the brain. (Högel et al., 2018) PET imaging is based on the interaction of ligands labelled with radioactive isotopes with specific targets for example in CNS. When the radioactive isotopes emit positrons, the amount of the ligand binding can be detected with gamma counter inside PET camera after an intravenous injection of labelled ligand. (Zanzonico, 2012).

Brain PET imaging targets in MS includes reactive astrocytes, neurons, myelin, and microglia. Mitochondrial 18-kDa translocator protein (TSPO) is the most widely used target in the PET imaging of neuroinflammation and microglial activation. (Högel et al., 2018) TSPO, also known as peripheral benzodiazepine receptor (PBR) is expressed at low levels on microglia in

healthy brain but in response to pathogens and insults, TSPO-radioligand signal increases due to the increased density of the cells and due to upregulation of microglia and macrophage proinflammatory activation (Airas and Yong, 2022). Additionally, according to recent evidence from *in vitro* and *in vivo* studied, increased expression of TSPO in neuroinflammation might be specific for proinflammatory microglia (Beckers et al., 2018). There are several radioligands targeting TSPO, but [^{11}C]PK11195 was the first, discovered in 1984, and it is still the most widely used ligand in TSPO-PET imaging (Airas and Yong, 2022). TSPO-PET image of MS brain using [^{11}C]PK11195 is presented in Figure 2.

Based on previous studies regarding MS disease, it is strongly suggested that microglial activation, which is central in the pathophysiology of MS, can be visualized with TSPO-PET (Ching et al., 2012). Diffuse pathology has previously been proven to be central in PMS pathology and associate with axonal damage in neuropathological study (Frischer et al., 2009). Using TSPO-PET, diffuse inflammation outside lesions can be detected *in vivo* (Sucksdorff et al., 2020). The fact that [^{11}C]PK11195-radioligand binding was increased in NAWM and normal appearing grey matter (NAGM) outside the lesions in patients with SPMS compared to patients with RRMS and HCs strengthens the assumption that functional change of microglia (activation) in MS brain is in a central role in MS pathology (Rissanen et al., 2014; Airas et al., 2015).

Importantly, several studies have shown that TSPO-PET imaging can be used as a prognostic marker for MS worsening independent of relapses and to detect the effect of MS therapeutics on microglial activation (Giannetti et al., 2014; Ratchford et al., 2012; Sucksdorff et al., 2017, 2019). Furthermore, microglial activation measured in the NAWM of MS patients has been shown to correlate with EDSS (Rissanen et al., 2014). In addition to white matter changes, increased microglial activation in the cortical grey matter has been suggested to be related to cognitive testing results in MS (Herranz et al., 2016). Additionally, there is evidence that structural and molecular brain changes measured with diffusion tensor imaging (DTI), measuring destruction of white matter fibers associates with microglial activity measured with TSPO-PET in NAWM in patients with MS (Bezukladova et al., 2020). This association between microglial activation and axonal injury is further demonstrated in a study, in which a relationship between increased innate immune cell activation and neurofilament light chain (NfL, described in Chapter 1.4.1), a biomarker for neuroaxonal damage, was found in patients with MS (Saraste et al., 2023). The strongest association with NfL was found between

microglial activation at the rim of chronic T1 hypointense lesions and in the perilesional NAWM and NfL. These results highlight the fact that microglial activation, especially within the perilesional NAWM and chronic lesion rim affect to neuroaxonal damage leading to the release of NfL (Saraste et al., 2023).

Since it has been found that ligand uptake is increased in gadolinium-positive focal lesions and decreased in chronic lesions, it has been hypothesized that TSPO-PET can be used to categorize lesions into phenotypes based on their microglial activity (Debruyne et al., 2003). Accordingly, an automated method has been developed to categorize chronic T1 lesions into rim-active, inactive, and overall active lesions based on innate immune cell activation patterns (proportion of TSPO-positive voxels) in lesion core and at the 2-mm perilesional rim (Nylund et al., 2022). In a study including 91 MS patients higher proportion of rim-active (smouldering) lesions associated with an increased EDSS score and more advanced brain atrophy (Nylund et al., 2022). Furthermore, by using the same method, Polvinen et al., found that the increased number of rim-active and decreased number of inactive lesions contributed to neurodegeneration in MS and can be used to detect disease progression *in vivo* (Polvinen et al., 2023).

Notwithstanding, there are limitations in TSPO-PET imaging. TSPO is also expressed in non-microglial cells such as macrophages, endothelial cells and astrocytes. This creates a problem since the brain is heavily vascularized and the signal coming from blood vessels needs to be removed. [^{11}C]PK11195-radioligand has a high specificity for TSPO but lamentably, it has a low signal-to-noise ratio which is related to the relatively low penetration through the BBB and its binding to endothelial and smooth muscle cells in brain. The biggest limitations in TSPO-PET imaging are related to the quality of the TSPO radioligands and post-processing methodology which is relatively time consuming and difficult to standardize making it difficult to compare the results between PET centers. In MS studies, one complicating factor is the lack of anatomically clearly defined reference region devoid of specific binding. (Airas et al., 2015) To overcome this weakness an automated method for the supervised clustering of normal grey matter reference for [^{11}C]PK11195 PET images has been developed (SuperPK software; Imperial College, London, UK) (Yaqub et al., 2012).

Above mentioned problems regarding [^{11}C]PK11195-ligand have been attempted to be solved by developing new tracers. These so-called second-generation tracers have higher specificity and signal-to-noise ratio, but they also have their own weaknesses. Subjects used in second-

generation tracer studies need to be genotyped because there are three phenotypes regarding the TSPO-binding affinity thus affecting the analysis of the results and inclusion criteria in these studies. (Owen et al., 2011) In addition to new TSPO-binding ligands, other imaging targets have been discovered. P2X7 receptor (P2X7R) and P2Y12 receptor (P2Y12R) are potential new targets that can be employed to measure microglia activity. The first is found in pro-inflammatory microglia in MS lesions and the latter in homeostatic microglia. (Airas and Yong, 2022)

In conclusion, PET imaging using radioligands binding to the TSPO on activated microglia provides an *in vivo* method to detect the microglial activation in NAWM and normal appearing grey matter (NAGM) and in lesions. The main reason, why TSPO-PET imaging is considered as more accurate imaging method especially in PMS is that MRI can only detect focal lesions whereas TSPO-PET captures diffuse inflammation and microglia related pathology in MS brain.

1.4 Liquid biomarkers in MS

Since the diagnosis of MS based on the brain histopathology of the disease is difficult, the diagnosis, separation into subtypes and treatment decisions are made based on symptoms, lesion progression in MRI, and changes in CSF sample. Additional liquid biomarkers would be beneficial not only in monitoring the disease progression but also in choosing effective therapies and discovering underlying cause of pathology since the disease is largely heterogenic. Moreover, imaging, especially PET, is expensive, time-consuming, and difficult to standardize; hence blood biomarkers would be needed.

CSF sample provides information about the inflammation in CNS and enables exclusion of some other diseases with symptoms alike (e.g., neuromyelitis optica spectrum disorder and acute disseminated encephalomyelitis) whose treatment differs from that of MS disease. CSF sample is not necessary in most cases, but in MS, it can show raised white cell count, IgG index, and IgG oligoclonal bands, which are currently the most established biomarkers predicting disability in MS patients. However, any of these CSF markers are not specific to MS and can be found in patients with other neuroinflammatory diseases. (Brownlee et al., 2017)

Since lumbar puncture is rather invasive procedure, several blood biomarkers have been investigated. Glial fibrillary acidic protein (GFAP) indicating glial dysfunction and

neurofilament light chain (NfL) indicating axonal damage are the most studied serum biomarkers in MS. A common finding is that NfL is more a marker of acute inflammation whereas GFAP, is rather a marker of disease progression. Markers of inflammation can also be detected in MS such as cytokines produced by pro-inflammatory cells, heat shock proteins regulating the immune responses, and ligand of CD40 positive lymphocytes (CD40L). Chitinase-3 like-protein-1 (CHI3L1)(Figure 3) is also a potential marker of inflammation, since it reflects microglial and astrocyte activity (Yang et al., 2022). One interesting new biomarker is sTREM-2, also a marker microglial activation (Azzolini et al., 2022). Other potential blood biomarkers include Nitric Oxide (NO) and S100β protein. The expression of NfL, GFAP and CHI3L1 in MS brain is presented in Figure 3.

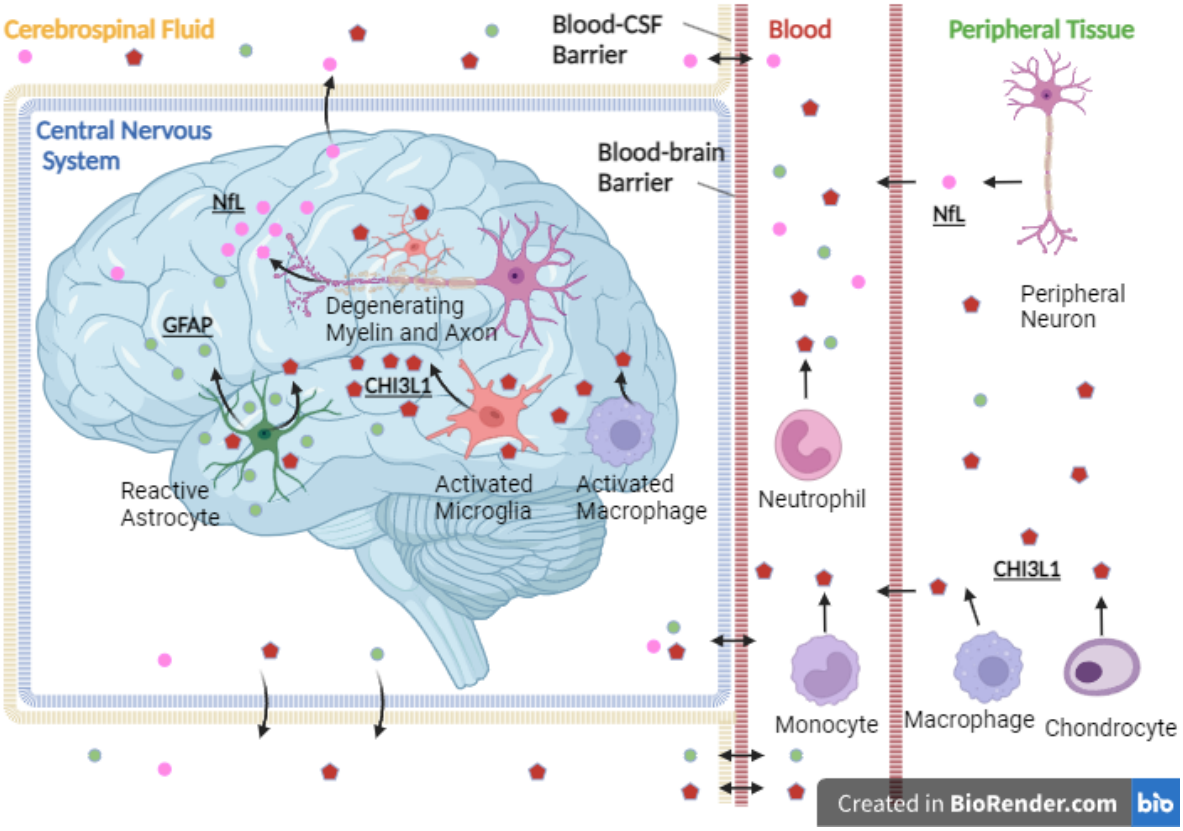

Figure 3. Liquid biomarkers GFAP, NfL and CHI3L1 in MS brain. GFAP is mainly released in CNS by activated astrocytes and NfL by degenerating axons. CHI3L1 is released in CNS both by microglia/macrophages and astrocytes. Additionally, CHI3L1 is released in periphery by monocytes, neutrophils, macrophages and chondrocytes but also by fibroblast-like cells, smooth muscle cells, and tumor cells. *CHI3L1, Chitinase-3 like-protein-1; CSF, Cerebrospinal fluid; GFAP, Glial fibrillary acidic protein; NfL; Neurofilament light chain. Figure is modified from* Gill et al., 2023. *Created in Biorender.*

1.4.1 NfL

NfL is the most widely studied CSF and blood biomarker in MS. NfL is a neurofilament protein synthesized in the soma of the nerve cells and it functions as part of their cytoskeleton. Neurofilaments participate in the growth and stability of axons and in maintaining mitochondrial stability and microtubule content. (Gafson et al., 2020) After axonal damage, neurofilaments are degraded by a calpain-mediated pathway leading to the release of neurofilament peptides into circulation (Norgren et al., 2004). Consequently, neurofilaments indicate axonal damage and neuronal injury and are effective in monitoring and predicting progression of various acute and chronic neurological diseases. Such neurological disorders include MS, dementia, stroke, traumatic brain injury (TBI), amyotrophic lateral sclerosis (ALS), and Huntington disease (Meeter et al., 2016; Gattringer et al., 2017; Shahim et al., 2016; Lu et al., 2015; Byrne et al., 2017).

A multitude of studies have demonstrated that serum NfL correlates with CSF NfL in MS disease indicating that blood levels relate to the pathology in brain (Disanto et al., 2017; Kuhle et al., 2016). While immunoblot, enzyme linked immunosorbent assay (ELISA), and electrochemiluminescence assays are relatively sensitive to detect CSF NfL, single-molecule array (SIMOA) is the most reliable assay to measure neurofilaments both in blood and in CSF samples (Khalil et al., 2018).

It has been shown that serum NfL was increased in MS patients compared to HCs (Disanto et al., 2017; Kuhle et al., 2016). Furthermore, serum levels can be employed to determine the presence of enhancing MRI lesions in MS brain thus indicating disease activity. Additionally, serum NfL levels have been proven to be associated with disability and relapse status, since the risk of future relapses and disability worsening is higher among patients with high serum levels of NfL. Also, the levels were found to associate with presence of relapses. Moreover, NfL can demonstrate treatment effects since DMT treated patients had lower serum NfL concentrations than untreated patients. (Disanto et al., 2017) It has been shown recently that serum NfL can be used to detect disease progression independent of relapses, although it's role as a liquid biomarker has previously been connected more to the acute damage rather than progressive (Meier et al., 2023; Bar-Or et al., 2023). Furthermore, a large cohort of 1421 RRMS and 596 PPMS patients showed that higher baseline NfL was prognostic for brain atrophy, increasing volume of slowly expanding lesions and clinical progression highlighting the role of blood NfL

as a marker of progressive disease (Bar-Or et al., 2023). Significantly, peripheral blood NfL concentrations have been used as an outcome measurement in phase 3 trials of fingolimod (Lublin et al., 2016) and ocrelizumab (Montalban et al., 2017) in PPMS (INFORMS and ORATORIO), and of siponimod (Kappos et al., 2018) and natalizumab (Kapoor et al., 2018) in SPMS (EXPAND and ASCEND).

1.4.2 GFAP

GPAP is a monomeric intermediate filament protein highly expressed in astrocytes in which it is a major part of cytoskeleton. The expression of GFAP in astrocytes is so specific that GFAP is widely used in immunohistochemistry in identifying astrocytes in post-mortem brain. (Gill et al., 2023) Activation of astrocytes and microglia in MS eventually leads to astrogliosis, which can be seen as the accumulation of GFAP in the MS brain eventually leading to release of GFAP from injured astrocytes into extracellular fluid, CSF and blood (Norgren et al., 2004). The most reliable assay to detect GFAP from circulation is SIMOA similarly to NfL.

Correlation between CSF and serum GFAP is high indicating that serum GFAP reflects CNS pathology reliably (Abdelhak et al., 2019). Higher serum concentrations of GFAP have been shown to associate with higher EDSS, older age, longer disease duration, progressive disease course and MRI pathology (Högel et al., 2020). Notably, it has also been demonstrated that GFAP is capable of predicting disease progression independent of relapses in a considerably large cohort (355 patients) and long follow-up period (7 years) (Meier et al., 2023). In addition, another study found that serum GFAP can be used to detect disability progression independent of relapses in patients undergoing treatment with ocrelizumab (Bar-Or et al., 2023). Despite these promising results, there are still varying results regarding the ability of GFAP to differentiate between healthy controls and MS patients and between PMS and RRMS patients. Also, the levels of GFAP tend to increase along with age, as is often the case with biomarkers, which makes it difficult to analyze the results as PMS patients are usually older. (Gill et al., 2023).

1.4.3 CHI3L1

Chitin is the second most substantial polysaccharide in nature. It is found in numerous organisms including arthropods, protozoan parasites, nematodes, bacteria, and fungi. (Elieh Ali Komi et al., 2018) Chitin synthetases and chitinases are in charge of chitin metabolism in chitin-

containing organisms. Although, mammals lack endogenous chitin and chitin synthases genes, they express true chitinases with enzymatic activity and homologous structurally related chitinase-like proteins (CLPs) that lack enzymatic activity due to a substitution of critical amino acids in the catalytic center but still bind to chitin. (Pinteac et al., 2021) In human, there are two true chitinases; chitotriosidase (CHIT1), and acidic mammalian chitinase (AMCase), and several CLPs; chitinase 3-like 2 (CHI3L2) ociductin-spesific glycoprotein (OCGP1), and stabilin-interacting CLP (SI-CLP) and CHI3L1, which is the most widely studied CLP. CHIT1 and CHI3L1 are expressed and secreted by macrophages and microglia. CHI3L2, expressed by cartilage chondrocytes and macrophages, has also been studied in neurologic disorders. Despite the physiologic and pathophysiologic roles of chitinases requires further investigation, they are considered as potential biomarkers in broad range of neurologic disorders. (Pinteac et al., 2021)

1.4.3.1 Expression

CHI3L1 (non-enzymatic chinase-3 like protein-1) is also named as YKL-40 because of its three N-terminal amino acids, tyrosine (Y), lysine (K), and leucine (L), and its molecular weight of 40 kDa. CHI3L1 is synthesized and secreted in periphery by macrophages, neutrophils, synoviocytes, chondrocytes, fibroblast-like cells, smooth muscle cells, and tumor cells. In brain, CHI3L1 is expressed by activated astrocytes and microglia.

In MS brain, the expression of CHI3L1 in both astrocytes and microglia has been studied widely. In brain autopsy samples of PMS patients , the expression of CHI3L1 was mainly seen by astrocytes in the rim of chronic active lesions, and in NAWM and NAGM whereas in RRMS, the expression was found both in astrocytes and microglia mostly in active lesions but also in NAWM (Cubas-Núñez et al., 2021). Furthermore, three studies found both astrocytes and microglia/ macrophages expressing CHI3L1 mostly in chronic active lesions but also in NAWM (Cantó et al., 2015b; Hinsinger et al., 2015; Ahmad et al., 2023). More precisely, it was found that CHI3L1 expression was more intense at the edge of the lesions and in the demyelinated area in chronic active lesions with high inflammatory activity (Cantó et al., 2015b). One study including RRMS patients found CHI3L1 expression in astrocytes only in lesions with high inflammatory activity, in which there were hypercellularity, abundant inflammatory infiltration around blood vessels and at the edge of the lesion, and active demyelination (Cantó et al., 2015b). Non-neurological control brain samples were negative for CHI3L1 staining (Cubas-Núñez et al., 2021). No expression of CHI3L1 was found in T

lymphocytes in paraffin-embedded brain samples of RRMS patient with CHI3L1 immunostaining (Cantó et al., 2015b).

1.4.3.2 Function

The function of CHI3L1 in inflammation and tissue repair has been studied widely in periphery. In tumor growth, CHI3L1 associated signaling has been connected into cancer cell growth, proliferation, invasion, metastasis, angiogenesis, activation of tumor associated macrophages, and Th2 polarization of CD4+ T cells (Zhao et al., 2020). Studies in arthritis, asthma, diabetes, liver fibrosis, coronary artery disease, and several cancers have already indicated that CHI3L1 is important in inflammatory processes and tissue remodeling (Johansen et al., 1999; Chupp et al., 2007; Rathcke et al., 2006; Tao et al., 2014; Schroder et al., 2020; Libreros et al., 2013). The expression of CHI3L1 is increased in the presence of pro-inflammatory cytokines such as IL-6, IFN-γ, IL-1β, and TNF-α *in vitro* in periphery in colonic epithelial cells, connective tissue cells, and in cancer cells; hence its role in inflammation is indisputable (Zhao et al., 2020; Mizoguchi, 2006; Ling and Recklies, 2004; Kzhyshkowska et al., 2006).

CHI3L1 binds to several receptors such as cancer associated IL-13Rα, TMEM219, CD44 and Galectin-3, and lung associated CRTH2. Moreover, CHI3L1 interacts with chitin, heparin, hyaluronic acid and collagen (Zhao et al., 2020). Signaling pathways include ERK1/2, PI3K, Wnt/β-catenin, FAK861/397, and MAPK and signaling depends widely on the cellular context. (Pinteac et al., 2021)

CHI3L1 regulates various functions central in neurodegenerative diseases such as oxidant injury, apoptosis, inflammasome activation, the Th1/Th2 inflammatory balance, M2 macrophage differentiation, dendritic cell accumulation, TGF-beeta1 expression, extracellular matrix regulation, and parenchymal scarring (Zhao et al., 2020). Additionally, dysfunction in the normal function of CHI3L1 has been linked to neurodegeneration since its concentration has been demonstrated to increase in several neurological diseases (Li et al., 2023). Importantly, increased expression of CHI3L1 has been shown to affect individual CNS cells; modulating microglia secretions and activation states, increasing neuronal death, and modifying oligodendrocyte precursor cell division (Connolly et al., 2023) In addition, CHI3L1 has been shown to affect dendritic cell accumulation in BRP-39 (mouse homologue of human CHI3L1) knockout mice (Lee et al., 2009). Since the neuroinflammatory processes in CNS, led by astrocytes and microglia, are similar to the innate inflammation in periphery, the findings in

periphery may be important considering the functions of CHI3L1 in brain because there is limited amount of evidence regarding the function in CNS (He et al., 2013; Choi et al., 2011; Connolly et al., 2023). In neuroinflammation, it has been proposed that CHI3L1 functions as a signaling molecule or as an effector in microglia-astrocyte-neuron axis by regulating microglia induced conversion of A1 reactive astrocytes further inducing neuronal death. This suggestion is based on the findings of CHI3L1 expression pattern in astrocytes and microglia. (Connolly et al., 2023) Moreover, it has been shown that CHI3L1 is able to modulate the microglial activation *in vitro* and *in vivo*. It has been shown *in vitro* that the expression of CHI3L1 in astrocytes is increased in the presence of pro-inflammatory mediators released from macrophages. Surprisingly, coculturing of astrocytes and microglia did not show inhibition of CHI3L1 expression in macrophages. (Bonneh-Barkay et al., 2012) The potential role of CHI3L1 in the function of individual CNS cells is presented in Figure 4.

The effects of CHI3L1 in the neuroinflammation have been studied *in vivo* using several mouse models. Ham et al., used an CHI3L1 inhibitor to see the effects in AD mouse model brain, and noticed that inhibition of CHI3L1 decreased M1 (pro-inflammatory microglia) markers TNFα, IL-1β and IL-6 thus inhibiting the activation of both microglia and astrocytes (Ham et al., 2020). In a cuprizone mouse model of PMS, in which there is toxic/metabolic demyelination and remyelination in different brain areas, the density of CHI3L1-positive cells had a strong relationship with microglial activation in the white matter and choroid plexus (Ahmad et al., 2023). However, Canto et al. found that there were no differences in gliosis nor disease course of EAE, a common mouse model of MS, between CHI3L1 knock-out mice and wild type mice although the expression of CHI3L1 was increased during the inflammatory phase of EAE (Cantó et al., 2015a).

Besides the role in neuroinflammation, there is also evidence for other functions of CHI3L1 in brain. It has been found that CHI3L1 is cytotoxic to neurons *in vitro* (Matute-Blanch et al., 2017). CHI3L1 may also physically associate with the BBB and act via the endothelial cells which is supported by its role in angiogenesis and vascular tissue remodeling in the periphery. Although CHI3L1 function in MS has been studied widely, further investigation is needed to uncover CHI3L1 signaling and its disease-specific roles. (Pinteac et al., 2021)

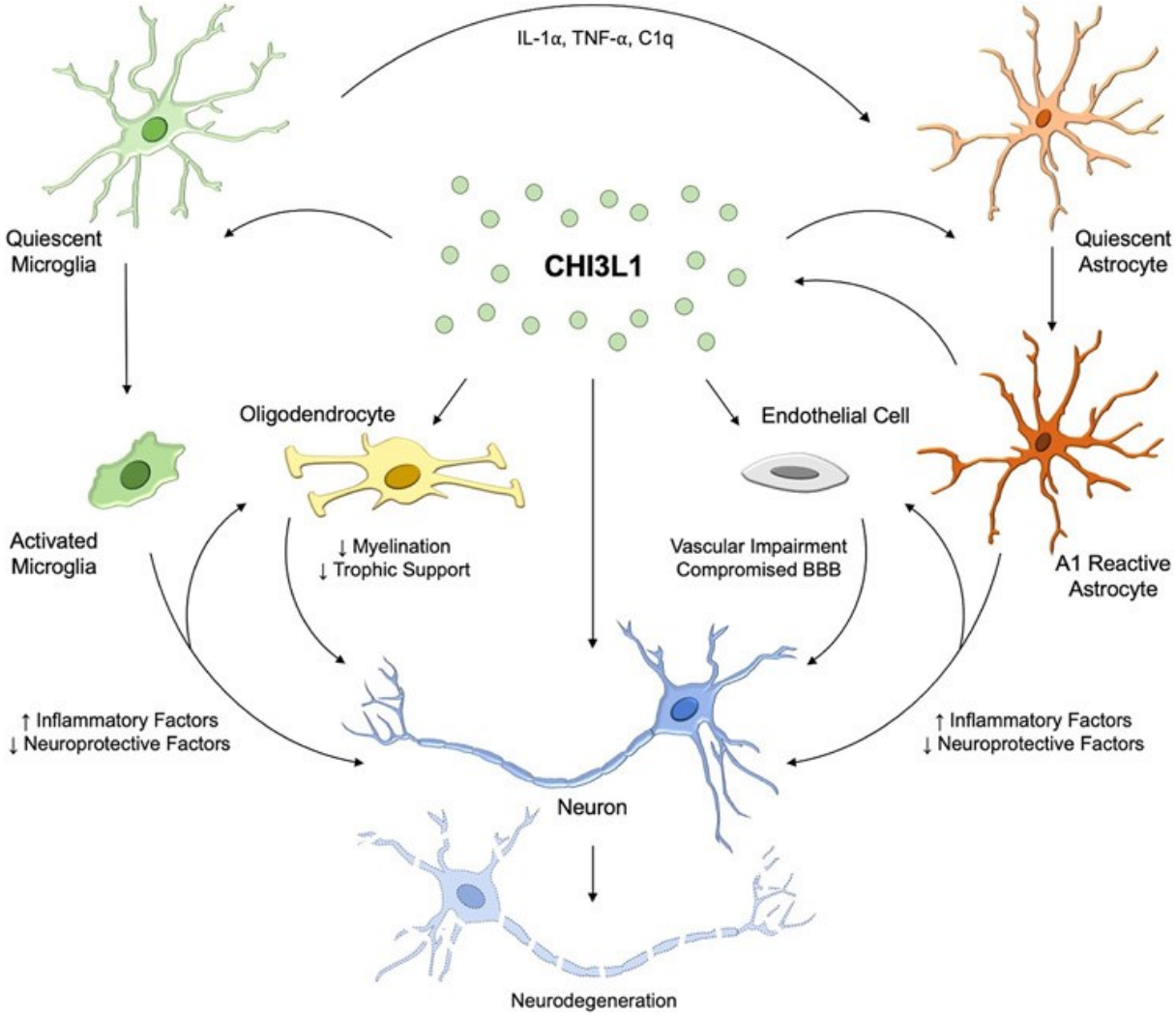

Figure 4. Potential role of CHI3L1 in CNS cells. CHI3L1 (Chitinase-3 like-protein-1) has been shown to affect individual CNS cells, microglia, astrocytes, oligodendrocytes, and endothelial cells in blood brain barrier. Based on previous research, it has been proposed that CHI3L1 functions as a signaling molecule between microglia and astrocytes. CHI3L1 also alters the glial activation and expression and secretion of inflammatory or neuroprotective factors. These actions may further affect oligodendrocytes and endothelial cells leading to demyelination and change in BBB function. Figure from Connolly et al., 2023.

1.4.3.3 Use as a biomarker in MS

In CSF, CHI3L1 is undeniably a pathophysiological biomarker reflecting inflammatory mechanisms in neurodegenerative diseases (Baldacci et al., 2017). A meta-analysis found that CSF CHI3L1 levels were higher in MS patients compared to healthy controls, higher in PPMS compared to RRMS and SPMS, and higher in CIS patients who converted to MS compared to those who did not (Floro et al., 2022).

There are several studies assessing CHI3L1 levels in peripheral blood of MS patients (Huss et al., 2020; Cantó et al., 2012; Cubas-Núñez et al., 2021; Lamancová et al., 2022; Fissolo et al., 2023; Hinsinger et al., 2015). Blood CHI3L1 has been studied also in other neurological diseases such as TBI, stroke, Alzheimer's disease, and ALS (Carabias et al., 2020; Xu et al., 2022; Choi et al., 2011; Vu et al., 2020; Cubas-Núñez et al., 2021). Huss et al., hypothesized that blood CHI3L1 might be a result of glial processes happening at the branches of astrocytes and astrocytic end feet, which constitute a part of the BBB and hence are in direct contact with blood vessels. Moreover, apoptosis and necrosis of astrocytes might release glial proteins, such as GFAP and CHI3L1 which are then released into blood via glymphatic system (Huss et al., 2020).

However, in MS, it has been debated whether serum CHI3L1 correlates with CSF CHI3L1, and it must be questioned whether blood CHI3L1 indicates elevated CHI3L1 levels in CNS or elevation in periphery since it is also produced by for example monocytes and synoviocytes. Hinsinger et al., found a high CSF/serum concentration ratio (approx. 8) which indicates that serum CHI3L1 arises mainly from intrathecal production in the brain and not from a systemic inflammation (Hinsinger et al., 2015). Another study also found similar results in CSF and serum of MS patients (Comabella et al., 2010). Nevertheless, one study found no correlations between serum and CSF CHI3L1 which they suggested was due to restricted diffusion through the brain extracellular space and across the BBB (Cubas-Núñez et al., 2021).

Despite these differing results considering CSF/blood CHI3L1 concentration ratio, several studies have found an increase in blood CHI3L1 in progressive forms of MS compared with RRMS and HCs (Cubas-Núñez et al., 2021; Lamancová et al., 2022; Cantó et al., 2012; Hinsinger et al., 2015). It has also been demonstrated that CIS patients with high CHI3L1 serum levels converted more rapidly to RRMS (Hinsinger et al., 2015). Still, some studies found no statistical differences between PMS, RRMS and HCs (Correale and Fiol, 2011).

Elevated CSF levels of CHI3L1 have been demonstrated to associate with higher risk and faster time for conversion from CIS to MS, faster development of disability, brain MRI lesions, and brain atrophy and may decrease upon disease-modifying (DMT) treatment (Gill et al., 2023; Cantó et al., 2015b). Interestingly, it has been discovered that a patient having ≥2 iron rims (vs. 0) had increased CSF CHI3L1 levels (Comabella et al., 2022).

It has been shown that there is a trend towards positive correlation between plasma CHI3L1 and clinical variables including number of relapses in the previous two years and EDSS at the time of blood sampling in a large, clinically diverse cohort of MS patients including 94 RRMS patients in remission, 30 in relapse, 32 IFNβ-treated, 30 SPMS and 66 PPMS patients. Similar results were observed, when RRMS patients were evaluated separately. However, correlations between plasma CHI3L1 and disease duration, number of relapses in the previous 2 years, and EDSS were not seen in SPMS and PPMS cohorts (Cantó et al., 2012). Conversely, Huss et al., found a correlation between EDSS and serum CHI3L1 only in PMS patients, not in RRMS patients (Huss et al., 2020). Additionally, Cubas-Nunez found no such correlations (Cubas-Núñez et al., 2021). Interestingly, Fissolo et al. found that the effect of serum CHI3L1 levels on disability outcomes in PPMS patients was clearly more noticeable in the short-term after 2 years, and remained as a trend in the long term (Fissolo et al., 2023).

During relapses, no alterations in plasma levels of CHI3L1 were found, although previously those alterations have been found in CSF (Cantó et al., 2012). Correlation between CHI3L1 plasma levels and a current MS treatment, IFNβ, has also been investigated. However, no statistically significant alterations in CHI3L1 plasma levels were found although the treatment tended to decrease the protein levels after treatment time of 8 months (Cantó et al., 2012).
Furthermore, positive correlations between CHI3L1 and other biomarkers such as GFAP and NfL have been studied. Fissolo et al., found that correlations between both NfL and GFAP were weak (Fissolo et al., 2023). Another study discovered a correlation between NfL and CHI3L1 only in SPMS group (Lamancová et al., 2022).

1.5 Aims and hypotheses

Based on the assumption that glial activation is more prominent driver of the disability in PMS than in RRMS, the levels of CHI3L1, a marker of glial activation, can be hypothesized to be increased especially in PMS patients. This has already been shown by multiple studies and CHI3L1 appears to be a promising biomarker indicating disease progression already from CIS to RRMS and further to progressive forms of MS. It has previously been shown that microglial activation is in key role in PMS pathology, but the question remains, how microglial activation and CHI3L1 in plasma samples of MS patients are connected. It is hypothesized that increased microglial activation correlates with increased plasma CHI3L1. Since there is a lack of MS therapies in PMS, there is an urgent need for new biomarkers that would be easily accessible and would measure underlying diffuse disease pathology; hence this study aiming to evaluate

the association between CHI3L1, and microglial activation measured with TSPO-PET would be valuable in measuring disease progression and underlying pathology in progressive MS disease.

2 Results

2.1 Characteristics of the study cohort

Study cohort was selected from MS patients and HCs, who have participated in previous research projects of Professor Laura Airas at Turku PET Centre in the years 2009-2023. All subjects had PET and MRI images taken and blood sample collected. MS patients participated also in clinical evaluation. Study cohort consisted of 71 study subjects of which 54 were MS patients and 17 were healthy controls. MS patients had been diagnosed with either progressive disease (SPMS n=21 and PPMS n= 4) or RRMS (n= 29). RRMS patients were further divided into two groups: active (n=14) and benign (n=15), based on their disease activity determined with time between last relapse and PET imaging and presence of gadolinium positive lesions. Active RRMS patients had had either a relapse less than one year prior PET imaging with or without relapse associated disease worsening or a gadolinium positive lesion.

The mean time between blood sampling and PET image of healthy controls was 168 days (range 0-797 days) and of MS patients 153 days (range 0-2753). The time between blood sampling and PET image of nine MS patients was over six months (range 239-2735). These nine MS patients were excluded from the correlation analyses where PET and MRI variables were compared to CHI3L1 concentration to avoid any bias. Additionally, 5 healthy controls and 8 MS patients did not have GFAP and NfL measured; hence these subjects were excluded from those biomarker analyses.

2.1.1 Clinical characteristics

As in MS disease in general, most of the MS patients were female (67%). Also, most of the healthy controls were women (65%). The mean age was similar in MS and HC (47.4 vs. 44.6, $p = 0.30$). However, PMS patients were older compared to RRMS patients ($p < 0.0001$) and their disease duration was longer ($p = 0.0016$). PMS patients had also higher median EDSS than RRMS patients ($p < 0.0001$).

Patients in RRMS benign group had longer disease duration than in active group ($p = 0.0095$) but ARR ($p = 0.0065$) and MSSS ($p < 0.0001$) were lower. Additionally, in active group, EDSS was higher than in benign group ($p < 0.0001$).

24 of MS patients received MS treatment (Treatments: rituximab [n = 8], natalizumab [n = 4], fingolimod [n = 3], teriflunomide [n = 7], glatiramer acetate [n = 2]) and 30 were untreated. The demographical and clinical characteristics of the study cohort are presented in Table 1.

2.1.2 Brain volumetric characteristics

There was a trend towards decreased brain volume in MS patients compared to HCs ($p = 0.069$) (Table 2). Brain volume was decreased in PMS compared to RRMS ($p = 0.012$). Furthermore, NAWM volume was decreased in both MS vs. HC ($p = 0.014$) and PMS vs. RRMS ($p = 0.0003$). Also, grey matter volume was decreased in MS vs. HC ($p = 0.019$) and in PMS vs. RRMS ($p = 0.0080$). Similarly, thalamus volume was decreased in MS vs. HC ($p = 0.0007$) and in PMS vs. RRMS ($p < 0.0001$). Additionally, lesion load was higher in PMS compared to RRMS patients ($p < 0.0001$). There was a difference between RRMS active and benign patients in grey matter cortex volume ($p = 0.039$). The brain MRI volumetric variables are presented in Table 2.

Table 1. Demographical and clinical characteristics of the study cohort.

	HC (n=17)	MS (n=54)	P-value*	PMS (n=25)	RRMS (n=29)	P-value*	RRMS active (n=14)	RRMS benign (n=15)	P-value*
Gender									
Female, n (%)	11 (65)	36 (67)		16 (64)	20 (69)		9 (64)	11 (73)	
Male, n (%)	6 (35)	18 (33)		9 (36)	9 (31)		5 (36)	4 (27)	
Age†	44.6 (9.3)	47.4 (9.7)	0.30	53.3 (9.3)	42.2 (6.6)	**<0.0001**	42.2 (5.8)	42.2 (7.4)	>0.99
BMI‡	24.9 (23.0-27.4)	26.4 (22.0-33.2)	0.29	22.5 (20.2-28.2)	29.3 (25.3- 35.3)	**0.0039**	28.5 (25.6-35.4)	29.8 (25-36.1)	0.95
Disease duration§		14.8 (8.8)		18.8 (8.5)	11.5 (7.7)	**0.0016**	7.8 (7.1)	14.9 (6.7)	**0.0095**
MSSS†		3.76 (1.31-6.52)		4.63 (3.52-7.44)	1.43 (0.67-5.36)	**0.0005**	5.36 (2.11-7.32)	0.78 (0.38-1.39)	**<0.0001**
ARR¶		0.30 (0.2-0.64)		0.30 (0.14-0.54)	0.30 (0.2-0.84)	0.30	0.70 (0.27-1.45)	0.25 (0.19-0.42)	**0.0065**
EDSS†		3 (1.88-5.13)		5.5(3.5-6.5)	2 (1-2.75)	**<0.0001**	2.75 (2.38-3.13)	1 (1-2)	**<0.0001**
Time between relapse and PET**		3.98 (0.86-8.21)		5.64 (3.07-8.73)	1.87 (0.55-7.38)	0.093	0.55 (0.34-1.22)	6.74 (2.16-9.02)	**<0.0001**
Treatment									
Untreated		30		14	16		8	8	
Treated		24		11	13		6	7	

* From comparison of last mentioned 2 groups (HC vs. MS, PMS vs. RRMS and RRMS active vs. RRMS benign) using T-test (two-tailed) or Mann-Whitney test, † At the time of blood sampling, ‡ At baseline, § From first symptoms to sampling, ¶ Before baseline PET, ** Time between last relapse and baseline PET imaging. *ARR, annualized relapse rate; BMI, body mass index; EDSS, Expanded Disease Status Scale; HC, healthy control; MS, multiple sclerosis; MSSS, Multiple Sclerosis Status Scale; PMS, Progressive Multiple Sclerosis; RRMS, relapsing-remitting multiple sclerosis.*

Table 2. Brain MRI volume characteristics of healthy controls and MS patients.

Volume (cm^3)	HC (n=17)	MS (n=54)	P-value*	PMS (n=25)	RRMS (n=29)	P-value*	RRMS active (n=14)	RRMS benign (n=15)	P-value*
Brain	1181 (103.7)	1122 (117.2)	0.069	1080 (113.6)	1159 (109.2)	**0.012**	1129 (92.9)	1187 (118.8)	0.16
NAWM†	484.0 (53.07)	439.6 (66.02)	**0.014**	406.4 (64.08)	468.1 (53.91)	**0.0003**	459.1 (53.24)	476.5 (54.98)	0.39
Grey matter cortex	455.2 (420.7-477.7)	413.9 (393.5-450)	**0.019**	405.3 (372.5-437.3)	432 (401.7-470)	**0.0080**	413.9 (393.1-451)	436.7 (429-481)	**0.039**
Thalamus	15.15 (1.100)	13.19 (2.191)	**0.0007**	11.8 (1.859)	14.39 (1.705)	**<0.0001**	13.99 (1.724)	14.76 (1.659)	0.23
T1 lesion		6.384 (1.731-15.78)		15.76 (7.214-28.51)	1.771 (1.191-3.848)	**<0.0001**	2.168 (1.277-6.608)	1.689 (1.171-2.893)	0.34

* From comparison of last mentioned 2 groups (HC vs. MS, PMS vs. RRMS and RRMS active vs. RRMS benign) using T-test (two-tailed) or Mann-Whitney test

† Normal appearing white matter, T2 lesions subtracted from white matter

HC, healthy control; MS, multiple sclerosis; NAWM, normal-appearing white matter; PMS, progressive MS; RRMS, relapsing-remitting MS

2.1.3 TSPO-PET

[^{11}C]PK11195-binding, measured as distribution volume ratio (DVR), was increased in the whole brain in PMS compared to RRMS (mean 1.21 vs. 1.18; p = 0.0001) as well as in the NAWM (1.25 vs. 1.18; p < 0.0001) (Figure 5, Table 3). In thalamus [^{11}C]PK11195 DVR was increased in PMS compared to RRMS (p = 0.0052) and in RRMS active compared to RRMS benign (p = 0.023). There were no differences in DVRs between HCs and MS patients in whole brain (p = 0.40) or other studied regions of interests.

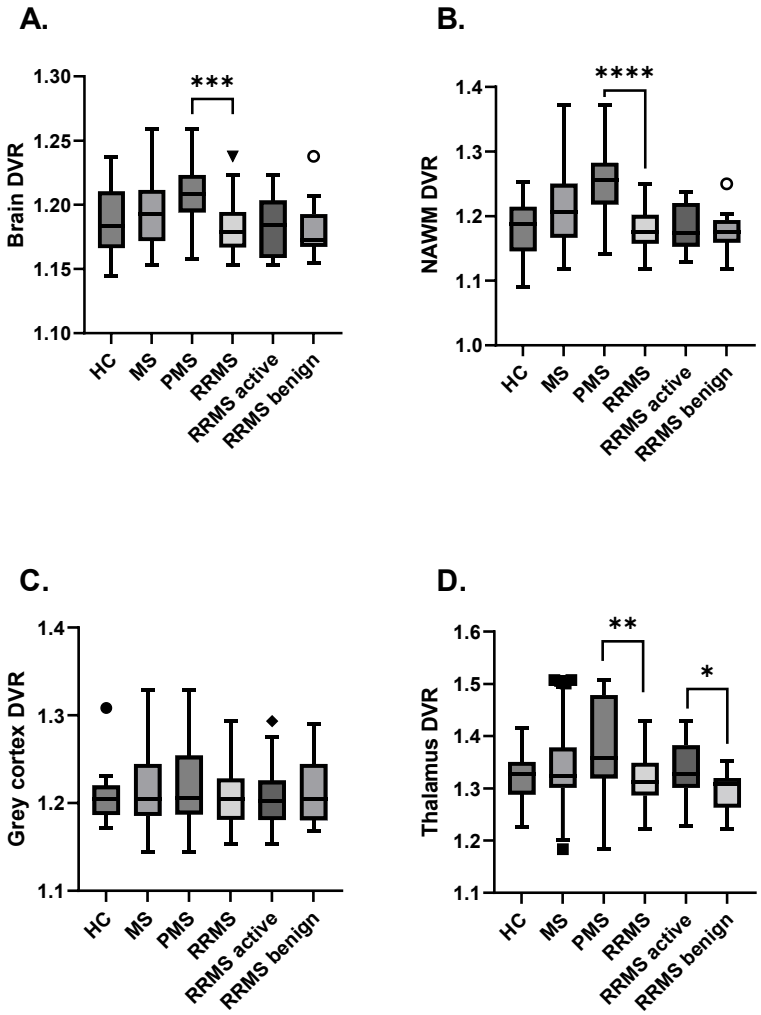

Figure 5. [^{11}C]PK11195 DVRs in MS patients and healthy controls. Microglial activity in different brain region of interests; brain, NAWM, cortical grey matter and thalamus, was measured with TSPO-PET using radioligand [^{11}C]PK11195. The amount of specific binding was measured as distribution volume ratio (DVR). *DVR, distribution volume ratio; HC, healthy control; MS, multiple sclerosis; NAWM, normal appearing white matter; PMS, progressive MS; RRMS, relapsing-remitting MS. * p<0.05, ** p<0.01, *** p<0.00*

Table 3. [^{11}C]PK11195 DVRs in MS patients and healthy controls.

	HC† (n=12)	MS‡ (n=51)	P-value*	PMS‡ (n=22)	RRMS (n=29)	P-value*	RRMS active (n=14)	RRMS benign (n=15)	P-value*
Brain DVR	1.18 (0.027)	1.19 (0.027)	0.40	1.21 (0.026)	1.18 (0.022)	**0.0001**	1.18 (0.023)	1.18 (0.022)	0.68
NAWM§ DVR	1.18 (0.048)	1.21 (0.055)	0.079	1.25 (0.050)	1.18 (0.033)	**<0.0001**	1.18 (0.036)	1.18 (0.031)	0.52
GM cortex DVR	1.20 (1.19-1.22)	1.20 (1.19-1.25)	0.86	1.21 (1.19-1.25)	1.20 (1.18-1.23)	0.29	1.20 (1.18-1.23)	1.20 (1.18-1.25)	0.95
Thalamus DVR	1.33 (1.29-1.35)	1.32 (1.30-1.38)	0.61	1.36 (1.32-1.48)	1.31 (1.29-1.35)	**0.0052**	1.33 (1.30-1.38)	1.31 (1.26-1.32)	**0.023**

* From comparison of last mentioned 2 groups (HC vs. MS, PMS vs. RRMS and RRMS active vs. RRMS benign) using T-test (two-tailed) or Mann-Whitney test
† 5 values missing
‡ 3 values missing
§ Normal appearing white matter, T2 lesions subtracted from white matter
DVR, distribution volume ratio; GM, Grey matter; HC, healthy control; MS, multiple sclerosis; NAWM, normal-appearing white matter; PMS, progressive MS; RRMS, relapsing-remitting MS

Microglial activity in MS lesions was not significantly increased in PMS compared to RRMS in whole lesions (T1 or T2). In contrast, in perilesional areas difference was observed. In PMS compared to RRMS, TSPO-binding was increased in T1 lesion rim 0-2mm ($p = 0.0042$) and in 2-6mm rim ($p < 0.0001$) (Figure 6, Table 4).

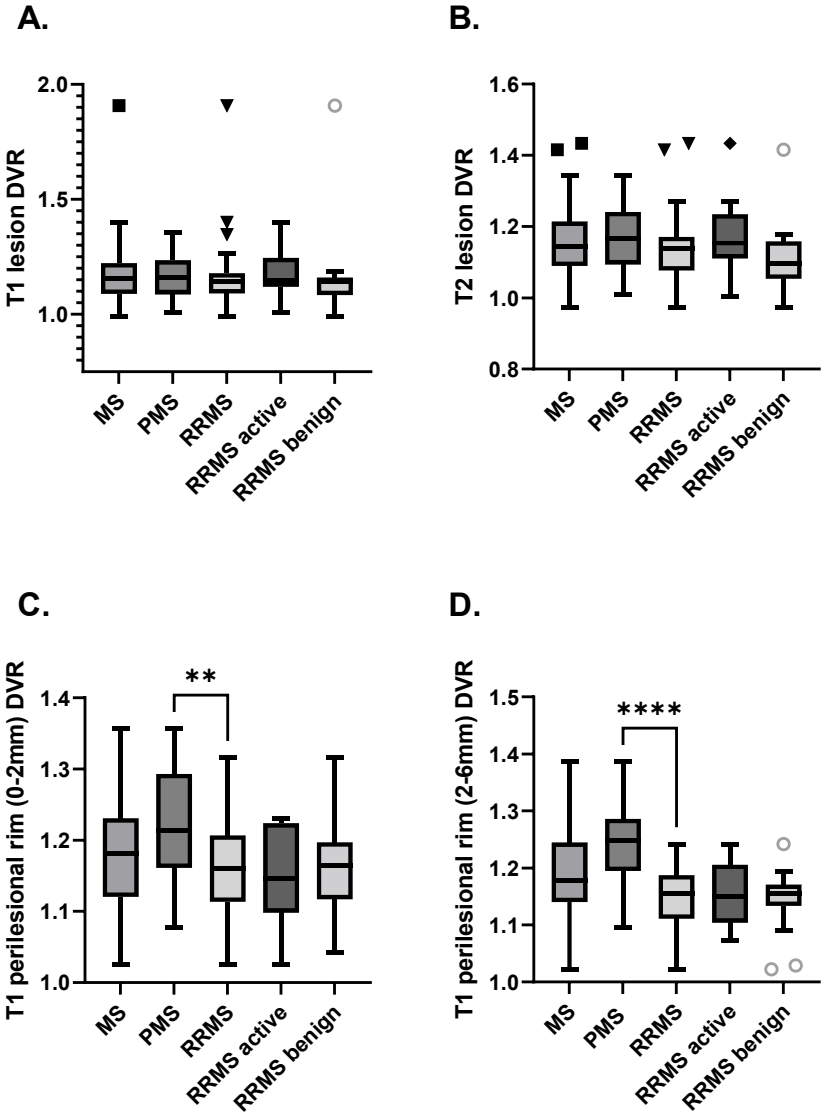

Figure 6. [^{11}C]PK11195 DVRs in lesions and perilesional areas of MS patients. Microglial activity in and around lesions: T1 lesion, T2 lesion, T1 perilesional rim (0-2 mm), and T1 perilesional rim (2-6 mm) was measured with TSPO-PET using radioligand [^{11}C]PK11195. The binding was measured as distribution volume ratio (DVR). *DVR, distribution volume ration; HC, healthy control; MS, multiple sclerosis; PMS, progressive MS; RRMS, relapsing-remitting MS. * $p<0.05$, ** $p<0.01$, *** $p<0.001$*

Table 4. [^{11}C]PK11195 DVRs in lesions and perilesional areas of MS patients.

DVR	MS† (n=51)	PMS† (n=22)	RRMS (n=29)	P-value*	RRMS active (n=14)	RRMS benign (n=15)	P-value*
T2 lesion	1.14 (1.09-1.21)	1.17 (1.09-1.24)	1.14 (1.08-1.17)	0.28	1.15 (1.11-1.23)	1.10 (1.05-1.16)	0.10
T1 perilesional area 0-2 mm	1.19 (0.08)	1.22 (0.09)	1.16 (0.07)	**0.0042**	1.15 (0.07)	1.17 (0.07)	0.54
T1 perilesional area 2-6 mm	1.19 (0.08)	1.24 (0.07)	1.15 (0.06)	**<0.0001**	1.15 (0.06)	1.14 (0.06)	0.62
T1 lesion	1.16 (1.09-1.22)	1.16 (1.09-1.24)	1.14 (1.09-1.18)	0.46	1.15 (1.12-1.25)	1.14 (1.08-1.16)	0.63

* From comparison of last mentioned 2 groups (PMS vs. RRMS and RRMS active vs. RRMS benign) using T-test (two-tailed) or Mann-Whitney test
† 3 values missing
DVR, distribution volume ration; HC, healthy control; MS, multiple sclerosis; PMS, progressive MS; RRMS, relapsing-remitting MS

When lesions were categorized into three groups according to [^{11}C]PK11195-binding, there were differences in rim-active, overall-active and inactive between PMS and RRMS patients. Number of rim-active lesions was significantly higher in PMS compared to RRMS ($p < 0.0001$) as well as the percentage of rim-active lesions ($p = 0.0001$) and volume of rim-active lesions ($p < 0.0001$). Additionally, number ($p < 0.0001$) and percentage ($p = 0.0011$) of overall-active lesions was higher in PMS compared to RRMS. On the other hand, the percentage of inactive-lesions was decreased in PMS compared to RRMS ($p < 0.0001$) (Table 5).

Table 5. Number, proportion and volume of TSPO-PET categorized lesion phenotypes in MS patients.

	MS† (n=51)	PMS† (n=22)	RRMS (n=29)	P-value*	RRMS active (n=14)	RRMS benign (n=15)	P-value*
Number of rim-active lesions	2 (0-6)	5 (3-8.25)	1 (0-2)	**<0.0001**	0.5 (0-3.25)	1 (0-2)	0.76
Number of overall-active lesions	9 (3-18)	18 (8.75-19.3)	6 (2-10)	**<0.0001**	6.5 (1.75-13)	3 (2-10)	0.54
Number of inactive lesions	6 (4-9)	6.5 (4.75-12)	6 (3-8)	0.46	7 (4.75-9.75)	5 (3-7)	0.13
% of rim-active lesions	12.5 (0-20)	19.8 (9.64-26.0)	6.25 (0-13.8)	**0.0001**	4.17 (0-14.4)	6.25 (0-14.3)	>0.9999
% of overall-active lesions	46.2 (33.3-57.1)	56.6 (48.2-60.6)	43.5 (26.8-48.1)	**0.0011**	41.8 (16.7-57.1)	43.5 (28.6-46.2)	0.92
% of inactive lesions	42.1 (23.1)	26.7 (16.4)	53.9 (20.6)	**<0.0001**	54.0 (23.4)	53.7 (18.5)	0.98
Volume of rim-active lesions	2.37 (0.76-13.4)	13.5 (5.05-19.1)	1.00 (0.12-2.26)	**<0.0001**	1.15 (0.091-3.72)	0.98 (0.13-1.20)	0.43
Volume of overall-active lesions	0.51 (0.28-0.84)	0.54 (0.35-0.81)	0.48 (0.22-0.84)	0.45	0.55 (0.29-0.93)	0.35 (0.17-0.76)	0.22
Volume of inactive lesions	2.82 (0-11.67)	3.63 (1.69-16.0)	0.82 (0-9.68)	**0.038**	1.56 (0-8.74)	0.82 (0-11.7)	0.99

* From comparison of last mentioned 2 groups (PMS vs. RRMS and RRMS active vs. RRMS benign) using T-test (two-tailed) or Mann-Whitney test
† 3 values missing
HC, healthy control; MS, multiple sclerosis; PMS, progressive MS; RRMS, relapsing-remitting MS.

2.2 Biomarker concentrations

Plasma CHI3L1 was increased in MS compared to HCs (median [IQR] 20.9 ng/ml [16.7-36.2] vs. 16.8 ng/ml [16.2-24.5]; p = 0.0497) when groups were compared in pairs shown in Table 6. Additionally, CHI3L1 was increased in PMS compared to HCs (23.5 (19.0-37.6) vs. 16.8 (16.2-24.5), p = 0.0055) (Figure 7, Table 6). There were no differences between PMS and RRMS (p = 0.0717) nor between RRMS active and benign (p = 0.75).

NfL concentration in serum was increased in MS patients compared to HCs (10.7 pg/ml [6.9-16.9] vs. 8.20 pg/ml [4.0-9.2]; p = 0.0064). Moreover, NfL concentration was increased in PMS compared to RRMS patients (8.6 pg/ml [6.7-13.8] vs. 5.0 pg/ml [10.0-22.6]; p = 0.031) and in RRMS active compared to RRMS benign (10.8 pg/ml [7.8-26.1] vs. 6.9 pg/ml [6.0-10.9]; p = 0.015) (Figure 7). Contrary to NfL, GFAP concentration was only increased in MS compared to HCs (107.8 pg/ml [70.5-138.8] vs. 55.5 pg/ml [43.7-85.5]; p = 0.0003) and in PMS compared to RRMS (137.8 pg/ml (99.1-194.7) vs. 75.8 pg/ml (64.2-124.7); p = 0.0024), but not in RRMS active compared to RRMS benign (p = 0.87) (Figure 7, Table 6).

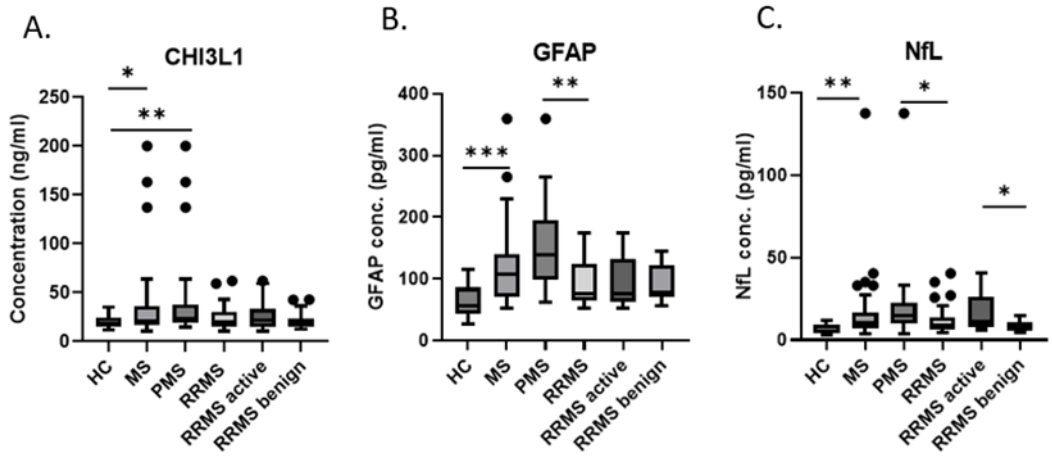

Figure 7. Biomarker concentrations in study cohort. A. Chitinase-3 like-protein-1 (CHI3L1) concentration (ng/ml) measured with ELISA from plasma. B. Glial fibrillary acidic protein (GFAP) concentration (pg/ml) measured with SIMOA from serum. C. Neurofilament light chain (NfL) concentration (pg/ml) measured with SIMOA from serum. *HC, healthy control; MS, multiple sclerosis; PMS, progressive MS; RRMS, relapsing-remitting MS. * p<0.05, ** p<0.01, *** p<0.001*

Table 6. Biomarker concentrations in study groups.

	HC (n= 17)	MS (n=54)	P-value*	PMS (n=25)	RRMS (n=29)	P-value*	RRMS active (n=14)	RRMS benign (n=15)	P-value*
NfL (pg/ml)†	8.20 (4.0-9.2)	10.7 (6.9-16.9)	**0.0064**	15.0 (10.0-22.6)	8.6 (6.7-13.8)	**0.0309**	10.8 (7.8-26.1)	6.9 (6.0-10.9)	**0.015**
GFAP (pg/ml)‡	55.5 (43.7-85.5)	107.8 (70.5-138.8)	**0.0003**	137.8 (99.1-194.7)	75.8 (64.2-124.7)	**0.0024**	75 (62.2-131.2)	78.2 (70.0-121.3)	0.87
CHI3L1 (ng/ml)	16.8 (16.2-24.5)	20.9 (16.7-36.2)	**0.0497**	23.5 (19.0-37.6)	19.8 (15.0-30.2)	0.0717	21.8 (14.6-33.0)	18.8 (14.9-23.5)	0.75

* From comparison of last mentioned 2 groups (HC vs. MS, PMS vs. RRMS and RRMS active vs. RRMS benign) using T-test (two-tailed) or Mann-Whitney test

† 5 HC and 8 PMS excluded from comparisons because missing value

‡ 5 HC and 8 PMS excluded from comparisons because missing value

GFAP, Glial fibrillary acidic protein; HC, healthy control; MS, multiple sclerosis; NfL, Neurofilament light chain; PMS, progressive MS; RRMS, relapsing-remitting MS

2.3 Correlations

2.3.1 Correlation between CHI3L1 and clinical and MRI variables

Correlation between CHI3L1 concentration and clinical and imaging data were assessed first in HCs (n = 17) and all MS patients (n = 54), and then separately in MS subgroups (PMS [n = 25], RRMS [n = 29], RRMS active [n = 14] and RRMS benign [n = 15]).

In HCs, there was a correlation between CHI3L1 concentration and age (r = 0.55, p = 0.023). There were no significant correlations between CHI3L1 concentration and MRI volumetric parameters in HCs (data not shown).

In whole MS group, there was a significant correlation between CHI3L1 concentration and age (r = 0.39, p = 0.0035). In addition, among all MS patients there was a trend towards positive correlation between CHI3L1 and EDSS (r = 0.27, p = 0.0508). In all MS patients CHI3L1 concentration correlated negatively with brain volume (r = -0.35, p = 0.020), cortical grey matter volume (r = -0.35, p = 0.019) and thalamus volume (r = -0.34, p = 0.022) (Table 7).

Remarkably, among PMS patients, CHI3L1 concentration did not correlate with age (r = 0.31, p = 0.13). Similarly to whole MS group, in PMS patients there was a negative correlation between CHI3L1 concentration and whole brain (r = -0.51, p = 0.021) and cortical grey matter volumes (r = -0.51, p = 0.045) (Table 7).

In RRMS patients CHI3L concentration correlated with age (r = 0.37, p = 0.047) and BMI (r = 0.56, p = 0.0015). There were no significant correlations between volumetric MRI variables and CHI3L1 concentration (Table 7). Similarly to whole RRMS group, there was a correlation with BMI in RRMS active (r = 0.64, p = 0.015) and with age RRMS benign (r = 0.59, p = 0.024) (data not shown). There were no significant correlations between volumetric MRI variables and CHI3L1 concentration in all in RRMS active and RRMS benign subgroups (data not shown).

Table 7. Correlations between plasma CHI3L1 concentration and clinical and MRI variables in all MS patients and in PMS and RRMS patients.

	MS (n = 54)		PMS (n = 25)		RRMS (n=29)	
	r	**p-value***	**r**	**p-value***	**r**	**p-value***
Age †	0.39	**0.0035**	0.31	0.13	**0.37**	**0.047**
BMI ‡	0.25	0.066	0.21	0.31	0.56	**0.0015**
Disease duration §	0.18	0.188	-0.14	0.50	0.19	0.33
MSSS †	0.14	0.32	0.080	0.72	0.078	0.69
ARR ¶	-0.028	0.84	0.014	0.95	-0.014	0.94
EDSS †	0.27	0.0508	0.010	0.96	0.20	0.29
Time between relapse and PET **	0.082	0.57	-0.097	0.67	0.18	0.34
GFAP (pg/ml) ††	0.10	0.51	-0.059	0.82	0.045	0.82
NfL (pg/ml) ††	0.20	0.18	0.23	0.36	0.12	0.53
NAWM volume ‡‡	-0.23	0.12	-0.49	0.056	-0.013	0.95
GM cortex volume ‡‡	-0.35	**0.019**	-0.51	**0.045**	-0.19	0.33
Thalamus volume ‡‡	-0.34	**0.022**	-0.44	0.091	-0.20	0.31
Brain volume ‡‡	-0.35	**0.020**	-0.58	**0.021**	-0.20	0.30
T1 hypo lesion load ‡‡	0.14	0.35	0.28	0.29	-0.12	0.55

* Spearman correlation, † At the time of blood sampling, ‡ At baseline. § From first symptoms to sampling, ¶ Before baseline PET, ** Time between last relapse and baseline PET imaging, †† 8 patients excluded from GFAP& NfL comparisons because their measurements are from different batch, ‡‡ 9 patients excluded because the time between imaging and blood sample was >6 months

ARR, annualized relapse rate; BMI, body mass index; GM, Grey matter; EDSS, Expanded Disease Status Scale; HC, healthy control; MS, multiple sclerosis; MSSS, Multiple Sclerosis Status Scale; NAWM, normal appearing white matter – White matter volume – T2 lesion volume; PMS, Progressive Multiple Sclerosis; RRMS, relapsing-remitting multiple sclerosis.

2.3.2 Correlation between CHI3L1 and TSPO-PET variables

When CHI3L1 concentration and [^{11}C]PK11195-binding presented as DVR in whole brain and different brain regions were compared in MS group, there was a correlation between brain DVR (r = 0.31, p = 0.049) and cortical grey matter DVR (r = 0.33, p = 0.032) and CHI3L1 concentration (Figure 8, Table 8).

Similarly to whole MS group, in PMS patients there was a correlation between CHI3L1 and brain DVR (r = 0.56, p = 0.0499) (Figure 8) but no significant correlations with other brain regions nor lesion DVRs. In whole RRMS group (Table 8) or in RRMS active and benign groups, there were no significant correlations between CHI3L1 concentration and brain DVRs.

There were no correlations between CHI3L1 and lesional or perilesional DVRs (Table 8), or lesion phenotypes (overall-active, rim-active and inactive) in any of the MS groups (data not shown).

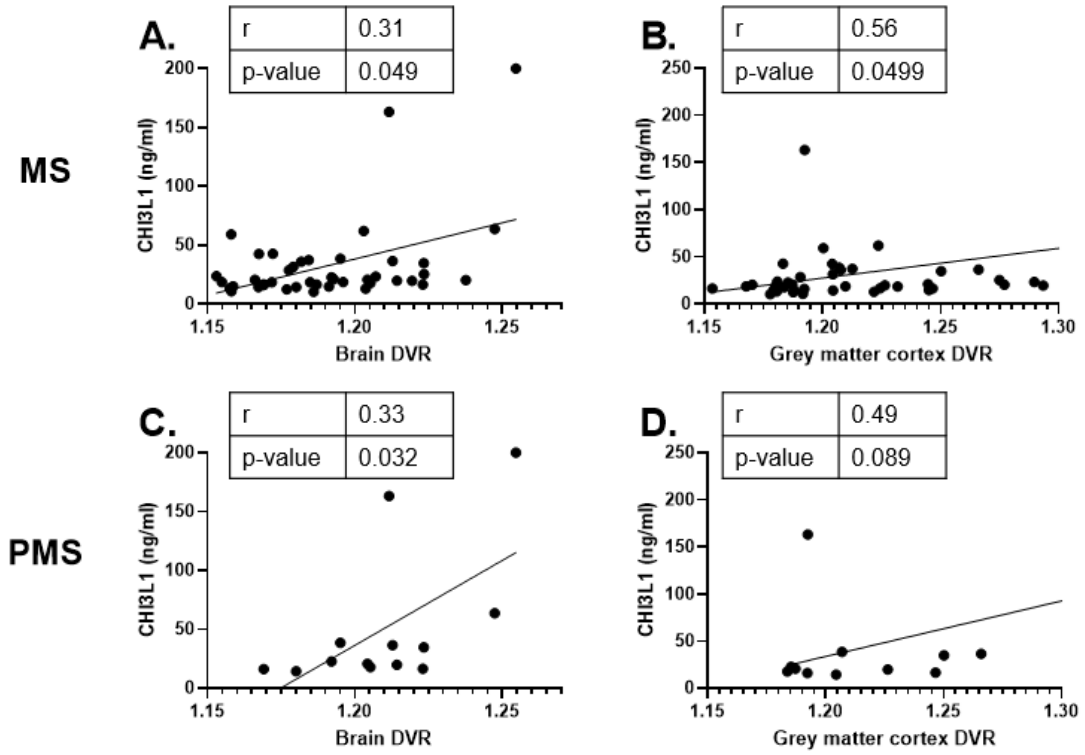

Figure 8. Correlation between CHI3L1 concentration and [^{11}C]PK11195-binding in all MS patients and in PMS patients. A.) Correlation between CHI3L1 concentration and Brain DVR in MS group (n=42). B.) Correlation between CHI3L1 concentration and cortical grey matter DVR in MS group (n=42). C.) Correlation between CHI3L1 concentration and Brain DVR in PMS group (n=13). D.) Correlation between CHI3L1 concentration and cortical grey matter DVR in PMS group (n=13). *DVR, Distribution volume ratio; MS, Multiple sclerosis; PMS, Progressive MS, r, Spearman correlation coefficient*

Table 8. CHI3L1 vs. DVR correlations in brain regions in MS, PMS and RRMS.

	MS (n = 42)		PMS (n = 13)		RRMS (n=29)	
	r	**p-value***	**r**	**p-value***	**r**	**p-value***
NAWM† DVR	0.085	0.59	0.10	0.74	-0.13	0.50
Brain DVR	0.31	**0.049**	**0.56**	**0.0499**	0.075	0.70
Cortical GM DVR	0.33	**0.032**	0.49	0.089	0.24	0.21
Thalamus DVR	0.081	0.61	-0.38	0.20	0.11	0.55
T2 DVR	-0.20	0.21	-0.038	0.91	-0.31	0.099
T1 perilesion 0-2 mm DVR	-0.096	0.55	0.18	0.55	-0.30	0.11
T1 perilesion 2-6 mm DVR	0.023	0.89	0.049	0.88	-0.20	0.31
T1 DVR	-0.18	0.25	0	>0.9999	-0.30	0.12

* Spearman correlation
† Normal appearing white matter, T2 lesions subtracted from white matter
DVR, distribution volume ratio; GM, Grey matter; HC, healthy control; MS, multiple sclerosis; NAWM, normal-appearing white matter; PMS, progressive MS; RRMS, relapsing-remitting MS

2.3.3 Correlation between CHI3L1 and other biomarkers (GFAP and NfL)

There were no significant correlations between CHI3L1 concentration and GFAP and NfL in HCs, whole MS group, PMS, RRMS, RRMS active or RRMS benign. However, when only those MS patients with CHI3L1 concentrations above the median CHI3L1 of MS patients (20.9 ng/ml) were considered, there was a strong correlation between CHI3L1 concentration and both GFAP ($r = 0.60$, $p = 0.0023$) and NfL ($r = 0.62$, $p = 0.0015$) (Figure 9).

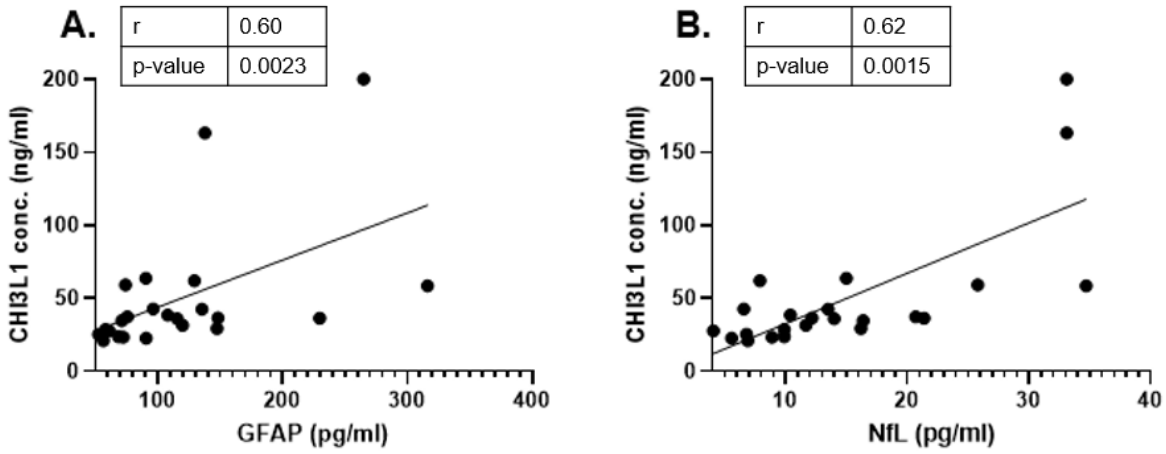

Figure 9. Biomarker correlations in CHI3L1 concentration high group. A. CHI3L1 concentration vs. GFAP concentration in CHI3L1 concentration high group (n=22). B. CHI3L1 concentration vs. NfL concentration in CHI3L1 concentration high group (n=22). CHI3L1 concentration was measured with ELISA and GFAP and NfL concentration with SIMOA. *CHI3L1, Chitinase-3 like-protein-1; GFAP, Glial fibrillary acidic protein; NfL; Neurofilament light chain; r, Spearman correlation coefficient.*

3 Materials and methods

3.1 Patient selection

MS patients were selected from an already existing patient cohort consisting of 130 MS patients (2009-2023) that have participated in the PET study, MRI, and clinical evaluation for EDSS score assessment. Imaging has been performed in Turku PET Centre and Turku University Hospital (TYKS). For the analyses, total of 71 subjects; 54 MS (both PMS and RRMS) and 17 HCs were selected (Figure 10). All study subjects had a blood sample taken and patients were diagnosed according to McDonald criteria (Thompson et al., 2018). RRMS patients were divided into two subgroups: benign and active. Patients in active RRMS group had had a relapse <1 year prior PET imaging with or without relapse associated worsening or a gadolinium positive lesion. Patients in benign RRMS group had EDSS score ≤ 2.5 and disease duration ≥ 8 years indicating the benign nature of their disease. Healthy controls with no known neurological symptoms or diseases were selected to match the MS cohort by their age and sex. Additionally, only study subjects who had a blood sample taken within 6 months of imaging (n= 42), were included in correlation analyses between CHI3L1 concentration and MRI- and PET-related variables.

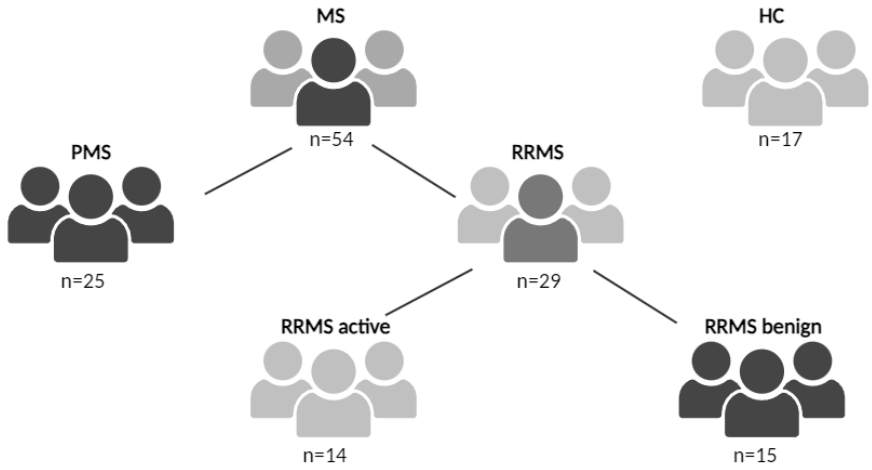

Figure 10. Study cohort. The study cohort consisted of 17 healthy controls and 54 MS patients of which 25 had PMS and 29 had RRMS. RRMS group was divided into active (n= 14) and benign group (n= 15) based on their disease activity measured as time between relapse and PET and presence of gadolinium positive lesions. *MS, Multiple sclerosis; HC, Healthy control; RRMS, Relapsing-remitting MS; PMS, Progressive MS*

3.2 Plasma sampling

Blood was collected into 10 ml Vacuette® serum clot-activator tubes (Greiner Bio-one, product number 455092) before 12 AM. Blood was allowed to coagulate for 30 min at room temperature, samples were centrifuged (2000 g, 10 min, RT), and plasma was frozen within 2 hours of sampling. Blood samples are stored in Auria Biobank (Turku, Finland) at -80 ℃ within 2 hours of sampling.

3.3 CHI3L1 ELISA quantification

The measurement of CHI3L1 plasma levels was conducted using quantitative sandwich enzyme immunoassay technique (Human Chitinase 3-like 1/YKL-40 Quantikine ELISA Kit, item number DC3L10, R&D Systems) following manufacturer's instructions. The minimum detectable dose of human CHI3L1 according to the kit was ranged from 1.25-8.15 pg/ml and the mean minimum detectable dose (MDD) was 3.55 pg/ml.

First, the dilutions 1:10, 1:50, 1:200 and 1:1000 were tested with 4 test samples (MS n=3, HC n=1). The selected dilution concentration for the actual analyses was 1:50 which was recommended by the manufacturer and the concentration coefficient of variation (CV%) of that dilution was low (1.7-3.2%). Optical densities were calculated with HIDEX Sense microplate reader (Hidex Oy, Turku, Finland) from the average of the duplicate readings for each standard, control, and sample of which the average zero standard optical density was subtracted.

Eight standards (4000 pg/ml, 2000 pg/ml, 1000 pg/ml, 500 pg/ml, 250 pg/ml, 62.5 pg/ml, and 0 pg/ml) were included in order to create a standard curve to calculate the concentration of CHI3L1 in plasma samples. A standard curve was created using four parameter logistic (4-PL) curve-fit with Origin 2016. Because in one plasma sample, the concentration was over the highest standard, but the optical density (OD) was close to the optical density of the highest standard the concentration was determined to be the same as the highest standard (200 ng/ml). The optical density was measured in wavelengths 450 and 570 and a variable (OD(450)-OD(570)).

3.4 MRI acquisition and analysis

MRI was conducted to gain an anatomical reference to PET images and to have volumetric data and to assess pathology related to MS. MRI scans of MS patients had already been performed at Turku PET Centre or at Turku University Central Hospital with either 3 T Ingenuity TF PET/MR System scanner (Philips Healthcare, Cleveland, Ohio, USA, n = 36) or 3T Ingenia (Philips, n = 35).

Axial T2, three-dimensional (3D) fluid-attenuated inversion recovery (FLAIR), 3DT1 and gadolinium-enhanced 3DT1 sequences with a spatial resolution of 1x1x1 mm were obtained. Eight patients lacked the gadolinium-enhanced 3DT1 sequences. MRI scans of HCs were performed in Turku, Finland with a Gyroscan Intera 1.5 T Nova Dual scanner, 3 T Ingenuity TF PET/MR System scanner or 3 T Ingenia scanner (Philips Healthcare). An 8-channel SENSE head coil was used in all MRI scans. A more detailed description of MRI methods has been explained previously (Bezukladova et al., 2020).

A semi-automated method including automated identification of T2 lesions followed by visual inspection and manual editing of the lesion masks was used to create a combined T2 lesion region of interest (ROI) and a combined T1 lesion ROI mask images to measure total lesion loads and determine NAWM and lesion associated ROIs. A detailed description of this method and creation of lesion rims has been made previously (Nylund et al., 2022). The brain ROI includes the cerebrum, cerebellum and brain stem, but excludes ventricles. The NAWM ROI was created by removing T2 lesion mask from the white matter ROI. Other ROIs used in both MRI and TSPO-PET were thalamus, cortical grey matter, T1 lesion, T2 lesion, T1 perilesional area (0-2 mm, [lesion rim]), T1 perilesional area (2-6 mm). Volumes of brain, NAWM, cortical grey matter, and lesions were obtained with Freesurfer software as previously described (Rissanen, 2018)

3.5 TSPO-PET acquisition and processing

PET scans (MS n = 51, HC n = 12) were performed with ECAT HRRT scanner (CTI/Siemens, resolution 2.5 mm) at Turku PET Centre as previously described (Nylund et al., 2022). For five healthy controls and three MS patients HRRT TSPO-PET was not available.

The tracer [^{11}C]PK11195 was used in PET scans. The radiochemical synthesis of [^{11}C]-(R)-PK11195 was performed with cyclotron in the Turku PET Centre following EU regulations. The details of synthesis has been described previously (Rissanen et al., 2014)(Rissanen et al., 2018). The mean of the injected dose was 470 (SD 53) MBq.

PET images have been post-processed and analyzed as previously described (Rissanen et al., 2018). DVR was calculated in specific ROIs (described in Chapter 3.4) using a supervised cluster algorithm (SuperPK software, SVCA4 classification) to assess the specific binding of [^{11}C]PK11195 (Turkheimer et al., 2007; Yaqub et al., 2012).

DVR was calculated in specific ROIs (described in Chapter 3.4) using a supervised cluster algorithm (SuperPK software, SVCA4 classification) to assess the specific binding of [^{11}C]PK11195 (Turkheimer et al., 2007; Yaqub et al., 2012). T1-hypointense lesions were divided into three different phenotypes; inactive (if no significant ligand binding was observed), overall-active (if the plaque had considerable ligand binding both in the core and at the rim), and rim-active (if the binding was low in the plaque core and considerably higher at the plaque edge) (Nylund et al., 2022).

3.6 Data collection

Required clinical, brain volumetric and PET-data was collected from Airasgroup-spreadsheet to a separate master's thesis excel sheet.

3.7 Statistical Methods

The standard curve of CHI3L1 plasma measurements was generated using Origin 2016 (four parameter logistic curve-fit, 4-PL) to calculate the concentrations of CHI3L1 in plasma samples using mean absorbance values.

Demographical, clinical and imaging data of the study cohort was analyzed using Graphpad Prism version 9.5.0 (GraphPad Software Inc., San Diego. CA). Normality of the data was tested using visual inspection, QQ plot and Shapiro-Wilk test where p-value <0.05 was considered as significant. Depending on the normality, either Unpaired t-test (assuming equal

variances/unequal variances) or Mann-Whitney test was used for group comparisons. Continuous variables are presented as median and quartiles (Q1 = 25% and Q3 = 75%) or mean and standard deviation depending on the normality of the data. Correlation was assessed using Spearman correlation since CHI3L1 concentration was not normally distributed.

3.8 Ethical and confidentiality issues

All study participants have signed a written consent form, and the participation is voluntary, and participants are able to withdraw from the trial at any time and without reason. All the data is securely stored for maintaining confidentiality and specific ID codes are used when analysing the data to avoid using patient information. The trial is approved by the ethics committee of Wellbeing Services County of South-West Finland (VARHA) and conducted by following instructions and guidelines given in the Declaration of Helsinki.

4 Discussion

MS disability progression is affected by multitude of alternating factors such as immune cell infiltration from the periphery, and microglia and astrocyte activation leading to diffuse inflammation. Focal and diffuse inflammation ultimately lead to demyelination and axonal damage seen as plaque formation and neurodegeneration throughout CNS. Diffuse inflammation and microglial activation can be detected *in vivo* with PET by measuring the amount of [^{11}C]PK11195-ligand binding to TSPO on microglial cells. CHI3L1 is a marker of neuroinflammation and is expressed by microglia and astrocytes and can be detected from peripheral blood of MS patients (Cantó et al., 2012). Therefore, the aim of this study was to evaluate the association between TSPO-PET measurable microglial activation and increased plasma concentration of CHI3L1. Additionally, the aim was to compare the levels of CHI3L1 to clinical and MRI data, and other previously measured biomarkers (GFAP and NfL). Regarding the fact that in previous studies blood CHI3L1 has been shown to be elevated in progressive MS disease (Cubas-Núñez et al., 2021; Lamancová et al., 2022; Cantó et al., 2012; Hinsinger et al., 2015), it was hypothesized that increased concentration of plasma CHI3L1 associates with microglial activation measured with TSPO-PET in multiple sclerosis since microglial activation has also been shown to correlate with disease progression (Giannetti et al., 2014; Ratchford et al., 2012; Sucksdorff et al., 2017, 2019).

This study confirms that the plasma concentration of CHI3L1 is increased in progressive forms of MS compared to healthy controls. The study also provides first evidence that there is an association between TSPO-PET measurable microglial activation in brain and plasma CHI3L1 concentration in MS and in PMS. Additionally, CHI3L1 concentration correlated with brain, cortical grey matter, and thalamus volumes in MS, and with cortical grey matter and brain volumes in PMS. In addition, there was a trend towards positive correlation between CHI3L1 concentration and EDSS in MS cohort.

As in previous studies (Cubas-Núñez et al., 2021; Cantó et al., 2012), CHI3L1 concentration was not affected by disease activity since there were no differences between RRMS active and benign groups. Furthermore, there were no correlations between CHI3L1 and ARR indicating the amount and occurrence of relapses. However, this might also be because of the relatively "mild" disease of RRMS active patients since the mean EDSS was 1.9 and only three patients had EDSS over 3.

Since the concentration of CHI3L1 was increased in PMS compared to HCs, CHI3L1 seems to be a marker for progressive disease. This has been already shown by multiple studies (Cubas-Núñez et al., 2021; Lamancová et al., 2022; Cantó et al., 2012; Hinsinger et al., 2015). This is supported by the fact that CHI3L1 concentration correlated with brain, cortical grey matter, and thalamus volume in MS cohort and with brain and cortical grey matter volume in PMS cohort. Moreover, the trend towards positive correlation between CHI3L1 concentration and EDSS in MS cohort strengthens this hypothesis. It has been previously shown that CHI3L1 correlates with EDSS in PMS patients (Huss et al., 2020) although there are varying results regarding this question since one study didn't find any correlation (Cubas-Núñez et al., 2021). In this study, there was no significant correlation between CHI3L1 concentration and EDSS in PMS patients which could be explained by a small cohort.

The age was similar in HCs compared to MS patients, but PMS patients were older compared to both RRMS patients and HCs which could affect the observed increase in the plasma of CHI3L1 in progressive patients. There was a strong correlation with age in the MS group, yet surprisingly not in PMS group. Still, these results must be further validated with older HC group and with regression model taking age into account to evaluate if increase in CHI3L1 levels in PMS group is due to higher age or increase in microglial activation.

The correlations between CHI3L1 and brain volume hasn't been studied much. In one study they didn't find significant correlation between CSF CHI3L1 and whole brain volume (Comabella et al., 2022). Interestingly, they found that CHI3L1 is associated with iron rims in patients with a first demyelinating event. This finding strengthens the assumption of CHI3L1 being a microglial marker since iron-rims contain mostly activated microglia whereas iron in astrocytes is mostly absent (Comabella et al., 2022). However, there was no evidence of association between CHI3L1 concentration and lesion load or microglial activation in lesions in the present study. Since there is strong evidence from histopathological studies (Cantó et al., 2015b; Hinsinger et al., 2015) that microglia derived CHI3L1 is found especially in MS lesions, this finding is surprising. Additionally the correlation between CSF CHI3L1 and T2 lesion volume has been previously shown (Comabella et al., 2022). Furthermore, despite pathological studies have indicated that in addition to lesions, CHI3L1 is expressed by microglia/macrophages located in NAWM (Cantó et al., 2015b; Hinsinger et al., 2015), there was no correlation between CHI3L1 concentration and microglial activation in NAWM. However, there was a correlation between CHI3L1 concentration and microglial activation in the whole brain of which NAWM comprises most.

Since in this study NfL correlated with CHI3L1 in those patients with high CHI3L1, the role of CHI3L1 in neurodegeneration can be hypothesized because NfL is specifically a marker for neurodegeneration. Additionally, the correlation between both GFAP and NfL in CHI3L1 high group highlights the hypothesis of the interaction of CHI3L1 with multiple cell types such as GFAP releasing astrocytes and NfL releasing neurons. However, higher age of these patients might affect the results since it is typical for biomarker concentrations to increase along with age. (Connolly et al., 2023). The relationship between serum CHI3L1 and other biomarkers has been studied previously. One study found a weak correlation between both serum GFAP and NfL and CHI3L1 in PPMS patients (Fissolo et al., 2023). Additionally, relationship between NfL and microglial activation has been studied previously (Saraste et al., 2023). According to that study the strongest associations were observed at the rim of chronic T1 hypointense lesions and in the perilesional NAWM and serum NfL. Although NfL is usually considered as a marker of disease activity this study reveals connection also in patients with no GD+ lesions or recent relapses which emphasizes the role of smouldering inflammation and its connection to increase in NfL concentration. This could explain the correlation between CHI3L1 concentration and NfL concentration. One interesting suggestion is to combine serum NfL, GFAP and CHI3L1 into a "Glia score" (CHI3L1*GFAP/NfL) which could help in monitoring the disease progression in MS. Huss et al., found that the glia score was higher in PMS patients compared to RRMS patients and correlated with EDSS when measured from serum in PMS group (Huss et al., 2020).

Most importantly, the correlation between increased CHI3L1 concentration and microglial activation measured with TSPO-PET both in MS and PMS cohorts indicates that CHI3L1 is a promising biomarker for MS progression-related smoldering inflammation. Additionally, this strengthens the assumption of the role of CHI3L1 in microglial activation. Furthermore, one study found that in PPMS patients without focal inflammatory activity, CHI3L1 predicted disease progression which indicates that in addition to neuroinflammation, CHI3L1 would recount neurodegeneration and diffuse inflammation. GFAP and NfL levels didn't predict disease progression in non-inflammatory patients (Fissolo et al., 2023). However, these results must be further studied.

This study has some limitations. Although, the role of TSPO-PET imaging in detecting activated microglia *in vivo* is well established, there are some challenges. It is not currently possible to differentiate between the anti-inflammatory (M2-type) and pro-inflammatory (M1-type) phenotypes of microglia with TSPO-targeting ligands, although this simple division of

microglia into two phenotypes (M1 and M2) has been debated (Ransohoff, 2016). It is also possible that detecting TSPO using PET imaging may illustrate the density of microglia/macrophages rather than their activation state (Airas et al., 2018). Still, it has been shown that TSPO-PET can be used to detect microglial activation promoting disease progression independent of relapses *in vivo* (Sucksdorff et al., 2020). Furthermore, studies on postmortem MS brain have shown that microglia in the NAWM have an activated morphology, and the number of homeostatic microglia that express homeostatic marker P2RY12 is reduced in MS patients compared to healthy individuals (Airas et al., 2018; Zrzavy et al., 2017). It is evident that age is a strong factor affecting both microglial activation and CHI3L1 concentration. This makes it more difficult to interpret the results although in the future, a statistic model that takes age into consideration could be created.

The CV% indicating the variation of the concentration in duplicate results was small suggesting that using CHI3L1 can be reliably measured using commercial ELISA-kit although measuring NfL and GFAP SIMOA-method is often used. In multiple previous studies, ELISA-method is also used when measuring blood CHI3L1 in MS patients (Cubas-Núñez et al., 2021; Huss et al., 2020; Correale and Fiol, 2011; Dönder and Özdemir, 2021; Lamancová et al., 2022; Cantó et al., 2012; Hinsinger et al., 2015). However, the question remains whether CSF and serum CHI3L1 correlate. CSF CHI3L1 has been proven in MS to elucidate well MS progression and correlate with clinical variables such as EDSS and brain volume loss (Cantó et al., 2015b; Floro et al., 2022). Blood CHI3L1 has been studied relatively little compared to GFAP and NfL although various studies have found elevated CHI3L1 levels in progressive patients (Cubas-Núñez et al., 2021; Lamancová et al., 2022; Cantó et al., 2012; Hinsinger et al., 2015). Since CHI3L1 is produced also in periphery, a question remains whether blood CHI3L1 arises from intrathecal production rather than from systemic inflammation. Controversial results have been obtained regarding this question. Hinsinger et al., found a high CSF/serum CHI3L1 concentration ratio (around eight) whereas Canto et al., didn't find same differences between MS subtypes both in CSF and serum samples (Hinsinger et al., 2015; Cantó et al., 2012). The correlation between CHI3L1 concentration and microglial activity in brain found in this study supports the assumption that CHI3L1 is derived from brain in MS and especially in PMS. Moreover, this is supported by the finding, that CHI3L1 correlates with GFAP and NfL in CHI3L1 high group.

Based on results presented here, one hypothesis could be that in those patients with considerably high CHI3L1 levels, CHI3L1 is mainly derived from brain and in those with little variation compared to healthy controls, the difference is caused by secretion of CHI3L1 from cells in periphery. This would mean that if a patient has considerably high levels of CHI3L1, the levels would predict disability progression. In this cohort of 54 MS patients, 3 patients had very high CHI3L1 concentration (>137 ng/ml vs. MS mean 34 ng/ml). All three patients had PMS (2 SMPS, 1 PPMS) and all had considerably high levels of GFAP and NfL also. Additionally, their brain DVR was high, brain volume low and lesion load high. These findings emphasize the role of CHI3L1 in disability progression although this must be further studied since only three patients had considerably high levels. This raises a question of which can be considered as normal variation in CHI3L1 levels and which level is considered as pathological mark indicating changes in brain.

The role of blood CHI3L1 in predicting MS disease progression needs to be further explored to overcome these above-mentioned problems. New biomarkers are urgently needed since progressive MS lacks effective treatment and clinical trials need reliable outcome measurements. It might be beneficial to combine CHI3L1 levels to GFAP and NfL or other potential markers of neuroinflammation and neurodegeneration since the disease is largely heterogenic. These results support the previous findings suggesting that CHI3L1 is a potential biomarker in MS and especially in PMS. In conclusion, correlation between CHI3L1 and microglial activation in brain suggests that CHI3L1 is a promising biomarker for MS progression-related smouldering inflammation.

5 Acknowledgements

I am extremely grateful to both my supervisors; Laura Airas, who made this thesis project possible and provided her knowledge and expertise, and Maija Saraste, who supported and guided me throughout the whole process and answered my almost daily questions. I would also like to express my thanks to my office colleagues and whole Airas Group, especially Marjo Nylund and Eveliina Honkonen both of whom supported me in all possible matters related both to the thesis and other matters. Also, I would like to express special thanks for Markus Matilainen, who helped me with the statistical analyses. Additionally, I am very grateful to Eeva-Christine Brockmann for all the practical help and Urpo Lamminmäki for enabling my laboratory work.

I am also grateful for my DDD classmates, family, friends, and my opponent for motivating and helping me during this process. Lastly, I would like to thank study participants without whom this study could not have been done.

6 Abbreviations

ALS	Amyotrophic lateral sclerosis
BBB	Blood-brain barrier
CHI3L1	Chitinase-3 like-protein-1
CIS	Clinically isolated syndrome
CLP	Chitinase-like protein
CNS	Central nervous system
CSF	Cerebrospinal fluid
DMT	Disease-modifying treatment
DVR	Distribution volume ratio
EAE	Experimental autoimmune encephalomyelitis
EBV	Epstein-Barr virus
EDSS	Expanded disability status scale
ELISA	Enzyme linked immunosorbent assay
FLAIR	Fluid-attenuated inversion recovery
GFAP	Glial fibrillary acidic protein
HC	Healthy control
HLA	Human leukocyte antigen
IRL	Iron rim lesion
MRI	Magnetic resonance imaging
MS	Multiple sclerosis
NAGM	Normal appearing grey matter
NAWM	Normal appearing white matter
NfL	Neurofilament light chain
PET	Positron emission tomography
PMS	Progressive MS
PPMS	Primary-progressive MS
PRL	Paramagnetic rim lesion
ROI	Region of interest
RRMS	Relapsing-remitting MS
SIMOA	Single-molecule array
SPMS	Secondary-progressive MS
TSPO	Mitochondrial 18-kDa translocator protein

References

Abdelhak, A., T. Hottenrott, E. Morenas-Rodríguez, M. Suárez-Calvet, U.K. Zettl, C. Haass, S.G. Meuth, S. Rauer, M. Otto, H. Tumani, and A. Huss. 2019. Glial Activation Markers in CSF and Serum From Patients With Primary Progressive Multiple Sclerosis: Potential of Serum GFAP as Disease Severity Marker? *Front. Neurol.* 10:280. doi:10.3389/fneur.2019.00280.

Absinta, M., P. Sati, F. Masuzzo, G. Nair, V. Sethi, H. Kolb, J. Ohayon, T. Wu, I.C.M. Cortese, and D.S. Reich. 2019. Association of Chronic Active Multiple Sclerosis Lesions With Disability In Vivo. *JAMA Neurol.* 76:1474–1483. doi:10.1001/jamaneurol.2019.2399.

Ahmad, I., S. Wergeland, E. Oveland, and L. Bø. 2023. An Association of Chitinase-3 Like-Protein-1 With Neuronal Deterioration in Multiple Sclerosis. *ASN Neuro*. 15:17590914231198980. doi:10.1177/17590914231198980.

Airas, L., M. Nylund, and E. Rissanen. 2018. Evaluation of Microglial Activation in Multiple Sclerosis Patients Using Positron Emission Tomography. *Front. Neurol.* 9:181. doi:10.3389/fneur.2018.00181.

Airas, L., E. Rissanen, and J.O. Rinne. 2015. Imaging neuroinflammation in multiple sclerosis using TSPO-PET. *Clin. Transl. imaging*. 3:461–473. doi:10.1007/s40336-015-0147-6.

Airas, L., and V.W. Yong. 2022. Microglia in multiple sclerosis - pathogenesis and imaging. *Curr. Opin. Neurol.* 35:299–306. doi:10.1097/WCO.0000000000001045.

Azzolini, F., L. Gilio, L. Pavone, E. Iezzi, E. Dolcetti, A. Bruno, F. Buttari, A. Musella, G. Mandolesi, L. Guadalupi, R. Furlan, A. Finardi, T. Micillo, F. Carbone, G. Matarese, D. Centonze, and M. Stampanoni Bassi. 2022. Neuroinflammation Is Associated with GFAP and sTREM2 Levels in Multiple Sclerosis. *Biomolecules*. 12. doi:10.3390/biom12020222.

Bagnato, F., P. Sati, C.C. Hemond, C. Elliott, S.A. Gauthier, D.M. Harrison, C. Mainero, J. Oh, D. Pitt, R.T. Shinohara, S.A. Smith, B. Trapp, C.J. Azevedo, P.A. Calabresi, R.G. Henry, C. Laule, D. Ontaneda, W.D. Rooney, N.L. Sicotte, D.S. Reich, and M. Absinta. 2024. Imaging chronic active lesions in multiple sclerosis: a consensus statement. *Brain*. doi:10.1093/brain/awae013.

Baldacci, F., S. Lista, E. Cavedo, U. Bonuccelli, and H. Hampel. 2017. Diagnostic function of the neuroinflammatory biomarker YKL-40 in Alzheimer's disease and other neurodegenerative diseases. *Expert Rev. Proteomics*. 14:285–299. doi:10.1080/14789450.2017.1304217.

Bar-Or, A., G.-A. Thanei, C. Harp, C. Bernasconi, U. Bonati, A.H. Cross, S. Fischer, L. Gaetano, S.L. Hauser, R. Hendricks, L. Kappos, J. Kuhle, D. Leppert, F. Model, A. Sauter, H. Koendgen, X. Jia, and A.E. Herman. 2023. Blood neurofilament light levels predict non-relapsing progression following anti-CD20 therapy in relapsing and primary progressive multiple sclerosis: findings from the ocrelizumab randomised, double-blind phase 3 clinical trials. *EBioMedicine*. 93:104662. doi:10.1016/j.ebiom.2023.104662.

Beckers, L., D. Ory, I. Geric, L. Declercq, M. Koole, M. Kassiou, G. Bormans, and M. Baes. 2018. Increased Expression of Translocator Protein (TSPO) Marks Pro-inflammatory Microglia but Does Not Predict Neurodegeneration. *Mol. imaging Biol.* 20:94–102. doi:10.1007/s11307-017-1099-1.

Bezukladova, S., J. Tuisku, M. Matilainen, A. Vuorimaa, M. Nylund, S. Smith, M. Sucksdorff, M. Mohammadian, V. Saunavaara, S. Laaksonen, J. Rokka, J.O. Rinne, E. Rissanen, and L. Airas. 2020. Insights into disseminated MS brain pathology with multimodal diffusion tensor and PET imaging. *Neurol. Neuroimmunol. neuroinflammation*. 7. doi:10.1212/NXI.0000000000000691.

Bjornevik, K., M. Cortese, B.C. Healy, J. Kuhle, M.J. Mina, Y. Leng, S.J. Elledge, D.W. Niebuhr, A.I.

Scher, K.L. Munger, and A. Ascherio. 2022. Longitudinal analysis reveals high prevalence of Epstein-Barr virus associated with multiple sclerosis. *Science*. 375:296–301. doi:10.1126/science.abj8222.

Bodini, B., M. Tonietto, L. Airas, and B. Stankoff. 2021. Positron emission tomography in multiple sclerosis - straight to the target. *Nat. Rev. Neurol.* 17:663–675. doi:10.1038/s41582-021-00537-1.

Bonneh-Barkay, D., S.J. Bissel, J. Kofler, A. Starkey, G. Wang, and C.A. Wiley. 2012. Astrocyte and macrophage regulation of YKL-40 expression and cellular response in neuroinflammation. *Brain Pathol.* 22:530–546. doi:10.1111/j.1750-3639.2011.00550.x.

Böttcher, C., M. van der Poel, C. Fernández-Zapata, S. Schlickeiser, J.K.H. Leman, C.-C. Hsiao, M.R. Mizee, Adelia, M.C.J. Vincenten, D. Kunkel, I. Huitinga, J. Hamann, and J. Priller. 2020. Single-cell mass cytometry reveals complex myeloid cell composition in active lesions of progressive multiple sclerosis. *Acta Neuropathol. Commun.* 8:136. doi:10.1186/s40478-020-01010-8.

Brownlee, W.J., T.A. Hardy, F. Fazekas, and D.H. Miller. 2017. Diagnosis of multiple sclerosis: progress and challenges. *Lancet (London, England)*. 389:1336–1346. doi:10.1016/S0140-6736(16)30959-X.

Byrne, L.M., F.B. Rodrigues, K. Blennow, A. Durr, B.R. Leavitt, R.A.C. Roos, R.I. Scahill, S.J. Tabrizi, H. Zetterberg, D. Langbehn, and E.J. Wild. 2017. Neurofilament light protein in blood as a potential biomarker of neurodegeneration in Huntington's disease: a retrospective cohort analysis. *Lancet. Neurol.* 16:601–609. doi:10.1016/S1474-4422(17)30124-2.

Cantó, E., C. Espejo, C. Costa, X. Montalban, and M. Comabella. 2015a. Breast regression protein-39 is not required for experimental autoimmune encephalomyelitis induction. *Clin. Immunol.* 160:133–141. doi:10.1016/j.clim.2015.06.004.

Cantó, E., F. Reverter, C. Morcillo-Suárez, F. Matesanz, O. Fernández, G. Izquierdo, K. Vandenbroeck, A. Rodríguez-Antigüedad, E. Urcelay, R. Arroyo, D. Otaegui, J. Olascoaga, A. Saiz, A. Navarro, A. Sanchez, C. Domínguez, A. Caminero, A. Horga, M. Tintoré, X. Montalban, and M. Comabella. 2012. Chitinase 3-like 1 plasma levels are increased in patients with progressive forms of multiple sclerosis. *Mult. Scler.* 18:983–990. doi:10.1177/1352458511433063.

Cantó, E., M. Tintoré, L.M. Villar, C. Costa, R. Nurtdinov, J.C. Álvarez-Cermeño, G. Arrambide, F. Reverter, F. Deisenhammer, H. Hegen, M. Khademi, T. Olsson, H. Tumani, E. Rodríguez-Martín, F. Piehl, A. Bartos, D. Zimova, J. Kotoucova, J. Kuhle, L. Kappos, J.A. García-Merino, A.J. Sánchez, A. Saiz, Y. Blanco, R. Hintzen, N. Jafari, D. Brassat, F. Lauda, R. Roesler, K. Rejdak, E. Papuc, C. de Andrés, S. Rauch, M. Khalil, C. Enzinger, D. Galimberti, E. Scarpini, C. Teunissen, A. Sánchez, A. Rovira, X. Montalban, and M. Comabella. 2015b. Chitinase 3-like 1: prognostic biomarker in clinically isolated syndromes. *Brain*. 138:918–931. doi:10.1093/brain/awv017.

Carabias, C.S., P.A. Gomez, I. Panero, C. Eiriz, A.M. Castaño-León, J. Egea, and A. Lagares. 2020. Chitinase-3-Like Protein 1, Serum Amyloid A1, C-Reactive Protein, and Procalcitonin Are Promising Biomarkers for Intracranial Severity Assessment of Traumatic Brain Injury: Relationship with Glasgow Coma Scale and Computed Tomography Volumetry. *World Neurosurg.* 134:e120–e143. doi:10.1016/j.wneu.2019.09.143.

Chataway, J., T. Williams, V. Li, R.A. Marrie, D. Ontaneda, and R.J. Fox. 2024. Clinical trials for progressive multiple sclerosis: progress, new lessons learned, and remaining challenges. *Lancet. Neurol.* 23:277–301. doi:10.1016/S1474-4422(24)00027-9.

Ching, A.S.C., B. Kuhnast, A. Damont, D. Roeda, B. Tavitian, and F. Dollé. 2012. Current paradigm of the 18-kDa translocator protein (TSPO) as a molecular target for PET imaging in

neuroinflammation and neurodegenerative diseases. *Insights Imaging*. 3:111–119. doi:10.1007/s13244-011-0128-x.

Choi, J., H.-W. Lee, and K. Suk. 2011. Plasma level of chitinase 3-like 1 protein increases in patients with early Alzheimer's disease. *J. Neurol.* 258:2181–2185. doi:10.1007/s00415-011-6087-9.

Chupp, G.L., C.G. Lee, N. Jarjour, Y.M. Shim, C.T. Holm, S. He, J.D. Dziura, J. Reed, A.J. Coyle, P. Kiener, M. Cullen, M. Grandsaigne, M.-C. Dombret, M. Aubier, M. Pretolani, and J.A. Elias. 2007. A chitinase-like protein in the lung and circulation of patients with severe asthma. *N. Engl. J. Med.* 357:2016–2027. doi:10.1056/NEJMoa073600.

Comabella, M., M.A. Clarke, S. Schaedelin, M. Tintoré, D. Pareto, N. Fissolo, R. Pinteac, C. Granziera, J. Sastre-Garriga, P. Benkert, C. Auger, J. Kuhle, X. Montalban, and A. Rovira. 2022. CSF chitinase 3-like 1 is associated with iron rims in patients with a first demyelinating event. *Mult. Scler.* 28:71–81. doi:10.1177/13524585211010082.

Comabella, M., M. Fernández, R. Martin, S. Rivera-Vallvé, E. Borrás, C. Chiva, E. Julià, A. Rovira, E. Cantó, J.C. Alvarez-Cermeño, L.M. Villar, M. Tintoré, and X. Montalban. 2010. Cerebrospinal fluid chitinase 3-like 1 levels are associated with conversion to multiple sclerosis. *Brain*. 133:1082–1093. doi:10.1093/brain/awq035.

Connolly, K., M. Lehoux, R. O'Rourke, B. Assetta, G.A. Erdemir, J.A. Elias, C.G. Lee, and Y.-W.A. Huang. 2023. Potential role of chitinase-3-like protein 1 (CHI3L1/YKL-40) in neurodegeneration and Alzheimer's disease. *Alzheimers. Dement.* 19:9–24. doi:10.1002/alz.12612.

Correale, J., and M. Fiol. 2011. Chitinase effects on immune cell response in neuromyelitis optica and multiple sclerosis. *Mult. Scler.* 17:521–531. doi:10.1177/1352458510392619.

Cubas-Núñez, L., S. Gil-Perotín, J. Castillo-Villalba, V. López, L. Solís Tarazona, R. Gasqué-Rubio, S. Carratalá-Boscá, C. Alcalá-Vicente, F. Pérez-Miralles, H. Lassmann, and B. Casanova. 2021. Potential Role of CHI3L1+ Astrocytes in Progression in MS. *Neurol. Neuroimmunol. neuroinflammation*. 8. doi:10.1212/NXI.0000000000000972.

Dal-Bianco, A., G. Grabner, C. Kronnerwetter, M. Weber, R. Höftberger, T. Berger, E. Auff, F. Leutmezer, S. Trattnig, H. Lassmann, F. Bagnato, and S. Hametner. 2017. Slow expansion of multiple sclerosis iron rim lesions: pathology and 7 T magnetic resonance imaging. *Acta Neuropathol.* 133:25–42. doi:10.1007/s00401-016-1636-z.

Datta, G., A. Colasanti, N. Kalk, D. Owen, G. Scott, E.A. Rabiner, R.N. Gunn, A. Lingford-Hughes, O. Malik, O. Ciccarelli, R. Nicholas, L. Nei, M. Battaglini, N. De Stefano, and P.M. Matthews. 2017. (11)C-PBR28 and (18)F-PBR111 Detect White Matter Inflammatory Heterogeneity in Multiple Sclerosis. *J. Nucl. Med.* 58:1477–1482. doi:10.2967/jnumed.116.187161.

Debruyne, J.C., J. Versijpt, K.J. Van Laere, F. De Vos, J. Keppens, K. Strijckmans, E. Achten, G. Slegers, R.A. Dierckx, J. Korf, and J.L. De Reuck. 2003. PET visualization of microglia in multiple sclerosis patients using [11C]PK11195. *Eur. J. Neurol.* 10:257–264. doi:10.1046/j.1468-1331.2003.00571.x.

Dendrou, C.A., L. Fugger, and M.A. Friese. 2015. Immunopathology of multiple sclerosis. *Nat. Rev. Immunol.* 15:545–558. doi:10.1038/nri3871.

Disanto, G., C. Barro, P. Benkert, Y. Naegelin, S. Schädelin, A. Giardiello, C. Zecca, K. Blennow, H. Zetterberg, D. Leppert, L. Kappos, C. Gobbi, and J. Kuhle. 2017. Serum Neurofilament light: A biomarker of neuronal damage in multiple sclerosis. *Ann. Neurol.* 81:857–870. doi:10.1002/ana.24954.

Dönder, A., and H.H. Özdemir. 2021. Serum YKL-40 levels in patients with multiple sclerosis. *Arq. Neuropsiquiatr.* 79:795–798. doi:10.1590/0004-282X-ANP-2020-0326.

Elieh Ali Komi, D., L. Sharma, and C.S. Dela Cruz. 2018. Chitin and Its Effects on Inflammatory and Immune Responses. *Clin. Rev. Allergy Immunol.* 54:213–223. doi:10.1007/s12016-017-8600-0.

Fissolo, N., P. Benkert, J. Sastre-Garriga, N. Mongay-Ochoa, A. Vilaseca-Jolonch, S. Llufriu, Y. Blanco, H. Hegen, K. Berek, F. Perez-Miralles, K. Rejdak, L.M. Villar, E. Monreal, R. Alvarez-Lafuente, O.K. Soylu, A. Abdelhak, F. Bachhuber, H. Tumani, S. Martínez-Yélamos, A.J. Sánchez-López, A. García-Merino, L. Gutiérrez, T. Castillo-Trivino, J. Lycke, I. Rosenstein, R. Furlan, M. Filippi, N. Téllez, L. Ramió-Torrentà, J.D. Lünemann, H. Wiendl, S. Eichau, M. Khalil, J. Kuhle, X. Montalban, and M. Comabella. 2023. Serum biomarker levels predict disability progression in patients with primary progressive multiple sclerosis. *J. Neurol. Neurosurg. Psychiatry*. doi:10.1136/jnnp-2023-332251.

Floro, S., T. Carandini, A.M. Pietroboni, M.A. De Riz, E. Scarpini, and D. Galimberti. 2022. Role of Chitinase 3-like 1 as a Biomarker in Multiple Sclerosis: A Systematic Review and Meta-analysis. *Neurol. Neuroimmunol. neuroinflammation*. 9. doi:10.1212/NXI.0000000000001164.

Frischer, J.M., S. Bramow, A. Dal-Bianco, C.F. Lucchinetti, H. Rauschka, M. Schmidbauer, H. Laursen, P.S. Sorensen, and H. Lassmann. 2009. The relation between inflammation and neurodegeneration in multiple sclerosis brains. *Brain*. 132:1175–1189. doi:10.1093/brain/awp070.

Gafson, A.R., N.R. Barthélemy, P. Bomont, R.O. Carare, H.D. Durham, J.-P. Julien, J. Kuhle, D. Leppert, R.A. Nixon, R.O. Weller, H. Zetterberg, and P.M. Matthews. 2020. Neurofilaments: neurobiological foundations for biomarker applications. *Brain*. 143:1975–1998. doi:10.1093/brain/awaa098.

Gattringer, T., D. Pinter, C. Enzinger, T. Seifert-Held, M. Kneihsl, S. Fandler, A. Pichler, C. Barro, S. Gröbke, M. Voortman, L. Pirpamer, E. Hofer, S. Ropele, R. Schmidt, J. Kuhle, F. Fazekas, and M. Khalil. 2017. Serum neurofilament light is sensitive to active cerebral small vessel disease. *Neurology*. 89:2108–2114. doi:10.1212/WNL.0000000000004645.

Giannetti, P., M. Politis, P. Su, F. Turkheimer, O. Malik, S. Keihaninejad, K. Wu, R. Reynolds, R. Nicholas, and P. Piccini. 2014. Microglia activation in multiple sclerosis black holes predicts outcome in progressive patients: an in vivo [(11)C](R)-PK11195-PET pilot study. *Neurobiol. Dis.* 65:203–210. doi:10.1016/j.nbd.2014.01.018.

Gill, A.J., E.M. Schorr, S.P. Gadani, and P.A. Calabresi. 2023. Emerging imaging and liquid biomarkers in multiple sclerosis. *Eur. J. Immunol.* 53:e2250228. doi:10.1002/eji.202250228.

Ham, H.J., Y.S. Lee, J. Yun, D.J. Son, H.P. Lee, S.-B. Han, and J.T. Hong. 2020. K284-6111 alleviates memory impairment and neuroinflammation in Tg2576 mice by inhibition of Chitinase-3-like 1 regulating ERK-dependent PTX3 pathway. *J. Neuroinflammation*. 17:350. doi:10.1186/s12974-020-02022-w.

He, C.H., C.G. Lee, C.S. Dela Cruz, C.-M. Lee, Y. Zhou, F. Ahangari, B. Ma, E.L. Herzog, S.A. Rosenberg, Y. Li, A.M. Nour, C.R. Parikh, I. Schmidt, Y. Modis, L. Cantley, and J.A. Elias. 2013. Chitinase 3-like 1 regulates cellular and tissue responses via IL-13 receptor α2. *Cell Rep.* 4:830–841. doi:10.1016/j.celrep.2013.07.032.

Healy, L.M., J.A. Stratton, T. Kuhlmann, and J. Antel. 2022. The role of glial cells in multiple sclerosis disease progression. *Nat. Rev. Neurol.* 18:237–248. doi:10.1038/s41582-022-00624-x.

Hellings, N., M. Barée, C. Verhoeven, M.B. D'hooghe, R. Medaer, C.C. Bernard, J. Raus, and P. Stinissen. 2001. T-cell reactivity to multiple myelin antigens in multiple sclerosis patients and healthy controls. *J. Neurosci. Res.* 63:290–302. doi:10.1002/1097-4547(20010201)63:3<290::AID-JNR1023>3.0.CO;2-4.

Hemond, C.C., and R. Bakshi. 2018. Magnetic Resonance Imaging in Multiple Sclerosis. *Cold Spring Harb. Perspect. Med.* 8. doi:10.1101/cshperspect.a028969.

Herranz, E., C. Giannì, C. Louapre, C.A. Treaba, S.T. Govindarajan, R. Ouellette, M.L. Loggia, J.A. Sloane, N. Madigan, D. Izquierdo-Garcia, N. Ward, G. Mangeat, T. Granberg, E.C. Klawiter, C. Catana, J.M. Hooker, N. Taylor, C. Ionete, R.P. Kinkel, and C. Mainero. 2016. Neuroinflammatory component of gray matter pathology in multiple sclerosis. *Ann. Neurol.* 80:776–790. doi:10.1002/ana.24791.

Hinsinger, G., N. Galéotti, N. Nabholz, S. Urbach, V. Rigau, C. Demattei, S. Lehmann, W. Camu, P. Labauge, G. Castelnovo, D. Brassat, D. Loussouarn, M. Salou, D. Laplaud, O. Casez, J. Bockaert, P. Marin, and E. Thouvenot. 2015. Chitinase 3-like proteins as diagnostic and prognostic biomarkers of multiple sclerosis. *Mult. Scler.* 21:1251–1261. doi:10.1177/1352458514561906.

Högel, H., E. Rissanen, C. Barro, M. Matilainen, M. Nylund, J. Kuhle, and L. Airas. 2020. Serum glial fibrillary acidic protein correlates with multiple sclerosis disease severity. *Mult. Scler.* 26:210–219. doi:10.1177/1352458518819380.

Högel, H., E. Rissanen, A. Vuorimaa, and L. Airas. 2018. Positron emission tomography imaging in evaluation of MS pathology in vivo. *Mult. Scler.* 24:1399–1412. doi:10.1177/1352458518791680.

Howell, O.W., J.L. Rundle, A. Garg, M. Komada, P.J. Brophy, and R. Reynolds. 2010. Activated microglia mediate axoglial disruption that contributes to axonal injury in multiple sclerosis. *J. Neuropathol. Exp. Neurol.* 69:1017–1033. doi:10.1097/NEN.0b013e3181f3a5b1.

Huss, A., M. Otto, M. Senel, A.C. Ludolph, A. Abdelhak, and H. Tumani. 2020. A Score Based on NfL and Glial Markers May Differentiate Between Relapsing-Remitting and Progressive MS Course. *Front. Neurol.* 11:608. doi:10.3389/fneur.2020.00608.

Jäckle, K., T. Zeis, N. Schaeren-Wiemers, A. Junker, F. van der Meer, N. Kramann, C. Stadelmann, and W. Brück. 2020. Molecular signature of slowly expanding lesions in progressive multiple sclerosis. *Brain*. 143:2073–2088. doi:10.1093/brain/awaa158.

Johansen, J.S., M. Stoltenberg, M. Hansen, A. Florescu, K. Hørslev-Petersen, I. Lorenzen, and P.A. Price. 1999. Serum YKL-40 concentrations in patients with rheumatoid arthritis: relation to disease activity. *Rheumatology (Oxford).* 38:618–626. doi:10.1093/rheumatology/38.7.618.

Kapoor, R., P.-R. Ho, N. Campbell, I. Chang, A. Deykin, F. Forrestal, N. Lucas, B. Yu, D.L. Arnold, M.S. Freedman, M.D. Goldman, H.-P. Hartung, E.K. Havrdová, D. Jeffery, A. Miller, F. Sellebjerg, D. Cadavid, D. Mikol, and D. Steiner. 2018. Effect of natalizumab on disease progression in secondary progressive multiple sclerosis (ASCEND): a phase 3, randomised, double-blind, placebo-controlled trial with an open-label extension. *Lancet. Neurol.* 17:405–415. doi:10.1016/S1474-4422(18)30069-3.

Kappos, L., A. Bar-Or, B.A.C. Cree, R.J. Fox, G. Giovannoni, R. Gold, P. Vermersch, D.L. Arnold, S. Arnould, T. Scherz, C. Wolf, E. Wallström, and F. Dahlke. 2018. Siponimod versus placebo in secondary progressive multiple sclerosis (EXPAND): a double-blind, randomised, phase 3 study. *Lancet (London, England)*. 391:1263–1273. doi:10.1016/S0140-6736(18)30475-6.

Kawachi, I., and H. Lassmann. 2017. Neurodegeneration in multiple sclerosis and neuromyelitis optica. *J. Neurol. Neurosurg. Psychiatry*. 88:137–145. doi:10.1136/jnnp-2016-313300.

Khalil, M., C.E. Teunissen, M. Otto, F. Piehl, M.P. Sormani, T. Gattringer, C. Barro, L. Kappos, M. Comabella, F. Fazekas, A. Petzold, K. Blennow, H. Zetterberg, and J. Kuhle. 2018. Neurofilaments as biomarkers in neurological disorders. *Nat. Rev. Neurol.* 14:577–589.

doi:10.1038/s41582-018-0058-z.

Kooi, E.-J., E.M.M. Strijbis, P. van der Valk, and J.J.G. Geurts. 2012. Heterogeneity of cortical lesions in multiple sclerosis: clinical and pathologic implications. *Neurology*. 79:1369–1376. doi:10.1212/WNL.0b013e31826c1b1c.

Kuhle, J., C. Barro, G. Disanto, A. Mathias, C. Soneson, G. Bonnier, Ö. Yaldizli, A. Regeniter, T. Derfuss, M. Canales, M. Schluep, R. Du Pasquier, G. Krueger, and C. Granziera. 2016. Serum neurofilament light chain in early relapsing remitting MS is increased and correlates with CSF levels and with MRI measures of disease severity. *Mult. Scler.* 22:1550–1559. doi:10.1177/1352458515623365.

Kuhlmann, T., S. Ludwin, A. Prat, J. Antel, W. Brück, and H. Lassmann. 2017. An updated histological classification system for multiple sclerosis lesions. *Acta Neuropathol.* 133:13–24. doi:10.1007/s00401-016-1653-y.

Kurtzke, J.F. 1983. Rating neurologic impairment in multiple sclerosis: an expanded disability status scale (EDSS). *Neurology*. 33:1444–1452. doi:10.1212/wnl.33.11.1444.

Kzhyshkowska, J., S. Mamidi, A. Gratchev, E. Kremmer, C. Schmuttermaier, L. Krusell, G. Haus, J. Utikal, K. Schledzewski, J. Scholtze, and S. Goerdt. 2006. Novel stabilin-1 interacting chitinase-like protein (SI-CLP) is up-regulated in alternatively activated macrophages and secreted via lysosomal pathway. *Blood*. 107:3221–3228. doi:10.1182/blood-2005-07-2843.

Lamancová, P., P. Urban, J. Mašlanková, M. Rabajdová, and M. Mareková. 2022. Correlation of selected serum protein levels with the degree of disability and NEDA-3 status in multiple sclerosis phenotypes. *Eur. Rev. Med. Pharmacol. Sci.* 26:3933–3941. doi:10.26355/eurrev_202206_28962.

Lampron, A., A. Larochelle, N. Laflamme, P. Préfontaine, M.-M. Plante, M.G. Sánchez, V.W. Yong, P.K. Stys, M.-È. Tremblay, and S. Rivest. 2015. Inefficient clearance of myelin debris by microglia impairs remyelinating processes. *J. Exp. Med.* 212:481–495. doi:10.1084/jem.20141656.

Lassmann, H. 2018. Multiple Sclerosis Pathology. *Cold Spring Harb. Perspect. Med.* 8. doi:10.1101/cshperspect.a028936.

Lee, C.G., D. Hartl, G.R. Lee, B. Koller, H. Matsuura, C.A. Da Silva, M.H. Sohn, L. Cohn, R.J. Homer, A.A. Kozhich, A. Humbles, J. Kearley, A. Coyle, G. Chupp, J. Reed, R.A. Flavell, and J.A. Elias. 2009. Role of breast regression protein 39 (BRP-39)/chitinase 3-like-1 in Th2 and IL-13-induced tissue responses and apoptosis. *J. Exp. Med.* 206:1149–1166. doi:10.1084/jem.20081271.

Li, F., A. Liu, M. Zhao, and L. Luo. 2023. Astrocytic Chitinase-3-like protein 1 in neurological diseases: Potential roles and future perspectives. *J. Neurochem.* 165:772–790. doi:10.1111/jnc.15824.

Libreros, S., R. Garcia-Areas, and V. Iragavarapu-Charyulu. 2013. CHI3L1 plays a role in cancer through enhanced production of pro-inflammatory/pro-tumorigenic and angiogenic factors. *Immunol. Res.* 57:99–105. doi:10.1007/s12026-013-8459-y.

Ling, H., and A.D. Recklies. 2004. The chitinase 3-like protein human cartilage glycoprotein 39 inhibits cellular responses to the inflammatory cytokines interleukin-1 and tumour necrosis factor-alpha. *Biochem. J.* 380:651–659. doi:10.1042/BJ20040099.

Lu, C.-H., C. Macdonald-Wallis, E. Gray, N. Pearce, A. Petzold, N. Norgren, G. Giovannoni, P. Fratta, K. Sidle, M. Fish, R. Orrell, R. Howard, K. Talbot, L. Greensmith, J. Kuhle, M.R. Turner, and A. Malaspina. 2015. Neurofilament light chain: A prognostic biomarker in amyotrophic

lateral sclerosis. *Neurology*. 84:2247–2257. doi:10.1212/WNL.0000000000001642.

Lublin, F., D.H. Miller, M.S. Freedman, B.A.C. Cree, J.S. Wolinsky, H. Weiner, C. Lubetzki, H.-P. Hartung, X. Montalban, B.M.J. Uitdehaag, M. Merschhemke, B. Li, N. Putzki, F.C. Liu, D.A. Häring, and L. Kappos. 2016. Oral fingolimod in primary progressive multiple sclerosis (INFORMS): a phase 3, randomised, double-blind, placebo-controlled trial. *Lancet (London, England)*. 387:1075–1084. doi:10.1016/S0140-6736(15)01314-8.

Masuda, T., R. Sankowski, O. Staszewski, C. Böttcher, L. Amann, Sagar, C. Scheiwe, S. Nessler, P. Kunz, G. van Loo, V.A. Coenen, P.C. Reinacher, A. Michel, U. Sure, R. Gold, D. Grün, J. Priller, C. Stadelmann, and M. Prinz. 2019. Spatial and temporal heterogeneity of mouse and human microglia at single-cell resolution. *Nature*. 566:388–392. doi:10.1038/s41586-019-0924-x.

Matute-Blanch, C., J. Río, L.M. Villar, L. Midaglia, S. Malhotra, J.C. Álvarez-Cermeño, A. Vidal-Jordana, X. Montalban, and M. Comabella. 2017. Chitinase 3-like 1 is associated with the response to interferon-beta treatment in multiple sclerosis. *J. Neuroimmunol.* 303:62–65. doi:10.1016/j.jneuroim.2016.12.006.

Meeter, L.H., E.G. Dopper, L.C. Jiskoot, R. Sanchez-Valle, C. Graff, L. Benussi, R. Ghidoni, Y.A. Pijnenburg, B. Borroni, D. Galimberti, R.J. Laforce, M. Masellis, R. Vandenberghe, I. Le Ber, M. Otto, R. van Minkelen, J.M. Papma, S.A. Rombouts, M. Balasa, L. Öijerstedt, V. Jelic, K.M. Dick, D.M. Cash, S.R. Harding, M. Jorge Cardoso, S. Ourselin, M.N. Rossor, A. Padovani, E. Scarpini, C. Fenoglio, M.C. Tartaglia, F. Lamari, C. Barro, J. Kuhle, J.D. Rohrer, C.E. Teunissen, and J.C. van Swieten. 2016. Neurofilament light chain: a biomarker for genetic frontotemporal dementia. *Ann. Clin. Transl. Neurol.* 3:623–636. doi:10.1002/acn3.325.

Meier, S., E.A.J. Willemse, S. Schaedelin, J. Oechtering, J. Lorscheider, L. Melie-Garcia, A. Cagol, M. Barakovic, R. Galbusera, S. Subramaniam, C. Barro, A. Abdelhak, S. Thebault, L. Achtnichts, P. Lalive, S. Müller, C. Pot, A. Salmen, G. Disanto, C. Zecca, M. D'Souza, A. Orleth, M. Khalil, A. Buchmann, R. Du Pasquier, Ö. Yaldizli, T. Derfuss, K. Berger, M. Hermesdorf, H. Wiendl, F. Piehl, M. Battaglini, U. Fischer, L. Kappos, C. Gobbi, C. Granziera, C. Bridel, D. Leppert, A. Maleska Maceski, P. Benkert, and J. Kuhle. 2023. Serum Glial Fibrillary Acidic Protein Compared With Neurofilament Light Chain as a Biomarker for Disease Progression in Multiple Sclerosis. *JAMA Neurol.* 80:287–297. doi:10.1001/jamaneurol.2022.5250.

Mizoguchi, E. 2006. Chitinase 3-like-1 exacerbates intestinal inflammation by enhancing bacterial adhesion and invasion in colonic epithelial cells. *Gastroenterology*. 130:398–411. doi:10.1053/j.gastro.2005.12.007.

Montalban, X., S.L. Hauser, L. Kappos, D.L. Arnold, A. Bar-Or, G. Comi, J. de Seze, G. Giovannoni, H.-P. Hartung, B. Hemmer, F. Lublin, K.W. Rammohan, K. Selmaj, A. Traboulsee, A. Sauter, D. Masterman, P. Fontoura, S. Belachew, H. Garren, N. Mairon, P. Chin, and J.S. Wolinsky. 2017. Ocrelizumab versus Placebo in Primary Progressive Multiple Sclerosis. *N. Engl. J. Med.* 376:209–220. doi:10.1056/NEJMoa1606468.

Norgren, N., P. Sundström, A. Svenningsson, L. Rosengren, T. Stigbrand, and M. Gunnarsson. 2004. Neurofilament and glial fibrillary acidic protein in multiple sclerosis. *Neurology*. 63:1586–1590. doi:10.1212/01.wnl.0000142988.49341.d1.

Nylund, M., M. Sucksdorff, M. Matilainen, E. Polvinen, J. Tuisku, and L. Airas. 2022. Phenotyping of multiple sclerosis lesions according to innate immune cell activation using 18 kDa translocator protein-PET. *Brain Commun.* 4:fcab301. doi:10.1093/braincomms/fcab301.

Owen, D.R.J., R.N. Gunn, E.A. Rabiner, I. Bennacef, M. Fujita, W.C. Kreisl, R.B. Innis, V.W. Pike, R. Reynolds, P.M. Matthews, and C.A. Parker. 2011. Mixed-affinity binding in humans with 18-

kDa translocator protein ligands. *J. Nucl. Med.* 52:24–32. doi:10.2967/jnumed.110.079459.

Pinteac, R., X. Montalban, and M. Comabella. 2021. Chitinases and chitinase-like proteins as biomarkers in neurologic disorders. *Neurol. Neuroimmunol. neuroinflammation*. 8. doi:10.1212/NXI.0000000000000921.

Pukoli, D., and L. Vécsei. 2023. Smouldering Lesion in MS: Microglia, Lymphocytes and Pathobiochemical Mechanisms. *Int. J. Mol. Sci.* 24. doi:10.3390/ijms241612631.

Ransohoff, R.M. 2016. A polarizing question: do M1 and M2 microglia exist? *Nat. Neurosci.* 19:987–991. doi:10.1038/nn.4338.

Ratchford, J.N., C.J. Endres, D.A. Hammoud, M.G. Pomper, N. Shiee, J. McGready, D.L. Pham, and P.A. Calabresi. 2012. Decreased microglial activation in MS patients treated with glatiramer acetate. *J. Neurol.* 259:1199–1205. doi:10.1007/s00415-011-6337-x.

Rathcke, C.N., J.S. Johansen, and H. Vestergaard. 2006. YKL-40, a biomarker of inflammation, is elevated in patients with type 2 diabetes and is related to insulin resistance. *Inflamm. Res. Off. J. Eur. Histamine Res. Soc. ... [et al.]*. 55:53–59. doi:10.1007/s00011-005-0010-8.

Reich, D.S., C.F. Lucchinetti, and P.A. Calabresi. 2018. Multiple Sclerosis. *N. Engl. J. Med.* 378:169–180. doi:10.1056/NEJMra1401483.

Rissanen, E., J. Tuisku, J. Rokka, T. Paavilainen, R. Parkkola, J.O. Rinne, and L. Airas. 2014. In Vivo Detection of Diffuse Inflammation in Secondary Progressive Multiple Sclerosis Using PET Imaging and the Radioligand ^{11}C-PK11195. *J. Nucl. Med.* 55:939–944. doi:10.2967/jnumed.113.131698.

Rissanen, E., J. Tuisku, T. Vahlberg, M. Sucksdorff, T. Paavilainen, R. Parkkola, J. Rokka, A. Gerhard, R. Hinz, P.S. Talbot, J.O. Rinne, and L. Airas. 2018. Microglial activation, white matter tract damage, and disability in MS. *Neurol. Neuroimmunol. neuroinflammation*. 5:e443. doi:10.1212/NXI.0000000000000443.

Saraste, M., M. Matilainen, A. Vuorimaa, S. Laaksonen, M. Sucksdorff, D. Leppert, J. Kuhle, and L. Airas. 2023. Association of serum neurofilament light with microglial activation in multiple sclerosis. *J. Neurol. Neurosurg. Psychiatry*. 94:698–706. doi:10.1136/jnnp-2023-331051.

Schroder, J., J.C. Jakobsen, P. Winkel, J. Hilden, G.B. Jensen, A. Sajadieh, A. Larsson, J. Ärnlöv, M. Harutyunyan, J.S. Johansen, E. Kjøller, C. Gluud, and J. Kastrup. 2020. Prognosis and Reclassification by YKL-40 in Stable Coronary Artery Disease. *J. Am. Heart Assoc.* 9:e014634. doi:10.1161/JAHA.119.014634.

Shahim, P., M. Gren, V. Liman, U. Andreasson, N. Norgren, Y. Tegner, N. Mattsson, N. Andreasen, M. Öst, H. Zetterberg, B. Nellgård, and K. Blennow. 2016. Serum neurofilament light protein predicts clinical outcome in traumatic brain injury. *Sci. Rep.* 6:36791. doi:10.1038/srep36791.

Sucksdorff, M., M. Matilainen, J. Tuisku, E. Polvinen, A. Vuorimaa, J. Rokka, M. Nylund, E. Rissanen, and L. Airas. 2020. Brain TSPO-PET predicts later disease progression independent of relapses in multiple sclerosis. *Brain*. 143:3318–3330. doi:10.1093/brain/awaa275.

Sucksdorff, M., E. Rissanen, J. Tuisku, S. Nuutinen, T. Paavilainen, J. Rokka, J. Rinne, and L. Airas. 2017. Evaluation of the Effect of Fingolimod Treatment on Microglial Activation Using Serial PET Imaging in Multiple Sclerosis. *J. Nucl. Med.* 58:1646–1651. doi:10.2967/jnumed.116.183020.

Sucksdorff, M., J. Tuisku, M. Matilainen, A. Vuorimaa, S. Smith, J. Keitilä, J. Rokka, R. Parkkola, M. Nylund, J. Rinne, E. Rissanen, and L. Airas. 2019. Natalizumab treatment reduces microglial activation in the white matter of the MS brain. *Neurol. Neuroimmunol. neuroinflammation*.

6:e574. doi:10.1212/NXI.0000000000000574.

Tang, Y., and W. Le. 2016. Differential Roles of M1 and M2 Microglia in Neurodegenerative Diseases. *Mol. Neurobiol.* 53:1181–1194. doi:10.1007/s12035-014-9070-5.

Tao, H., J.-J. Yang, K.-H. Shi, C. Huang, L. Zhang, X.-W. Lv, and J. Li. 2014. The significance of YKL-40 protein in liver fibrosis. *Inflamm. Res. Off. J. Eur. Histamine Res. Soc. ... [et al.]*. 63:249–254. doi:10.1007/s00011-013-0698-9.

Thompson, A., and O. Ciccarelli. 2020. Towards treating progressive multiple sclerosis. *Nat. Rev. Neurol.* 16:589–590. doi:10.1038/s41582-020-00421-4.

Thompson, A.J., B.L. Banwell, F. Barkhof, W.M. Carroll, T. Coetzee, G. Comi, J. Correale, F. Fazekas, M. Filippi, M.S. Freedman, K. Fujihara, S.L. Galetta, H.P. Hartung, L. Kappos, F.D. Lublin, R.A. Marrie, A.E. Miller, D.H. Miller, X. Montalban, E.M. Mowry, P.S. Sorensen, M. Tintoré, A.L. Traboulsee, M. Trojano, B.M.J. Uitdehaag, S. Vukusic, E. Waubant, B.G. Weinshenker, S.C. Reingold, and J.A. Cohen. 2018. Diagnosis of multiple sclerosis: 2017 revisions of the McDonald criteria. *Lancet. Neurol.* 17:162–173. doi:10.1016/S1474-4422(17)30470-2.

Turkheimer, F.E., P. Edison, N. Pavese, F. Roncaroli, A.N. Anderson, A. Hammers, A. Gerhard, R. Hinz, Y.F. Tai, and D.J. Brooks. 2007. Reference and target region modeling of [11C]-(R)-PK11195 brain studies. *J. Nucl. Med.* 48:158–167.

Vu, L., J. An, T. Kovalik, T. Gendron, L. Petrucelli, and R. Bowser. 2020. Cross-sectional and longitudinal measures of chitinase proteins in amyotrophic lateral sclerosis and expression of CHI3L1 in activated astrocytes. *J. Neurol. Neurosurg. Psychiatry*. 91:350–358. doi:10.1136/jnnp-2019-321916.

Xu, T., K. Zhang, C. Zhong, Z. Zhu, X. Zheng, P. Yang, B. Che, Y. Lu, and Y. Zhang. 2022. Plasma Human Cartilage Glycoprotein-39 Is Associated With the Prognosis of Acute Ischemic Stroke. *J. Am. Heart Assoc.* 11:e026263. doi:10.1161/JAHA.122.026263.

Yamasaki, R., H. Lu, O. Butovsky, N. Ohno, A.M. Rietsch, R. Cialic, P.M. Wu, C.E. Doykan, J. Lin, A.C. Cotleur, G. Kidd, M.M. Zorlu, N. Sun, W. Hu, L. Liu, J.-C. Lee, S.E. Taylor, L. Uehlein, D. Dixon, J. Gu, C.M. Floruta, M. Zhu, I.F. Charo, H.L. Weiner, and R.M. Ransohoff. 2014. Differential roles of microglia and monocytes in the inflamed central nervous system. *J. Exp. Med.* 211:1533–1549. doi:10.1084/jem.20132477.

Yang, J., M. Hamade, Q. Wu, Q. Wang, R. Axtell, S. Giri, and Y. Mao-Draayer. 2022. Current and Future Biomarkers in Multiple Sclerosis. *Int. J. Mol. Sci.* 23. doi:10.3390/ijms23115877.

Yaqub, M., B.N.M. van Berckel, A. Schuitemaker, R. Hinz, F.E. Turkheimer, G. Tomasi, A.A. Lammertsma, and R. Boellaard. 2012. Optimization of supervised cluster analysis for extracting reference tissue input curves in (R)-[(11)C]PK11195 brain PET studies. *J. Cereb. blood flow Metab. Off. J. Int. Soc. Cereb. Blood Flow Metab.* 32:1600–1608. doi:10.1038/jcbfm.2012.59.

Zanzonico, P. 2012. Principles of nuclear medicine imaging: planar, SPECT, PET, multi-modality, and autoradiography systems. *Radiat. Res.* 177:349–364. doi:10.1667/rr2577.1.

Zhao, T., Z. Su, Y. Li, X. Zhang, and Q. You. 2020. Chitinase-3 like-protein-1 function and its role in diseases. *Signal Transduct. Target. Ther.* 5:201. doi:10.1038/s41392-020-00303-7.

Zrzavy, T., S. Hametner, I. Wimmer, O. Butovsky, H.L. Weiner, and H. Lassmann. 2017. Loss of "homeostatic" microglia and patterns of their activation in active multiple sclerosis. *Brain*. 140:1900–1913. doi:10.1093/brain/awx113.